Green Synthesis of TiO_2/CuO Nanocomposites using *Rosa Abyssinica Leaf* Extract for Photocatalytic Degradation of MB Dye Under Visible Light Source

Ayana Kassahun Melaku

A Thesis Submitted to the Department of Applied Chemistry
School of Applied Natural Science

Office of Graduate Studies
Adama Science and Technology University

September, 2024
Adama, Ethiopia

Green Synthesis of TiO_2/CuO Nanocomposite using *Rosa Abyssinica Leaf* Extract for Photocatalytic Degradation of MB Dye Under Visible Light Source

Ayana Kassahun Melaku

Advisor: Aschalew Tadesse (PhD)

A Thesis Submitted to the Department of Applied Chemistry
School of Applied Natural Science

Presented in Partial Fulfillment of the Requirement for the Degree of Master's in applied chemistry (Industrial Chemistry)

Office of Graduate Studies
Adama Science and Technology University

September, 2024
Adama, Ethiopia

Declaration

I hereby declare that this Master Thesis entitled "**Green Synthesis of TiO_2/CuO Nanocomposite using *Rosa Abyssinica Leaf* Extract for Photodegradation of MB Dye Under Visible Light**" is my original work. That is, it has not been submitted for the award of any academic degree, diploma, or certificate in any other university. All sources of materials that are used for this thesis have been duly acknowledged through citation.

________________________	______________________	_______________
Name of student	Signature	Date

Recommendation of Advisor

I, the advisor of this thesis, hereby certify that I have read the revised version of the thesis entitled "**Green Synthesis of TiO_2/CuO Nanocomposite using *Rosa Abyssinica Leaf* Extract for Photocatalytic degradation of MB Dye Under Visible Light Source**" prepared under my guidance by Ayana Kassahun Melaku submitted in partial fulfillment of the requirements for the degree of Master of Science in Applied Chemistry. Therefore, I recommend the submission of the revised version of the thesis to the department following the applicable procedures.

________________________	________________________	________________
Advisor	Signature	Date

Approval Page

I, the advisor of the thesis entitled "**Green Synthesis of TiO_2/CuO Nanocomposite using *Rosa Abyssinica Leaf* Extract for Photocatalytic Degradation of MB Dye Under Visible Light Source**" and developed by Ayana Kassahun hereby certify that the recommendation and suggestions made by the board of examiners are appropriately incorporated into the final version of the thesis.

______________________	______________________	______________
Advisor	Signature	Date

Approval of the Board of Reviewers

We, the undersigned, members of the Board of Examiners of the thesis by Ayana Kassahun have read and evaluated the thesis entitled "**Green Synthesis of TiO_2/CuO Nanocomposite using *Rosa Abyssinica Leaf* Extract for Photocatalytic Degradation of MB Dye Under Visible Light Source**" and examined the candidate during open defense. This is, therefore, to certify that the thesis is accepted for partial fulfillment of the requirement of the degree of Master of Science in Applied Chemistry.

______________________	____________	______________
Chairperson	Signature	Date
______________________	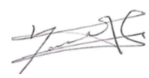 ____________	______________
Reviewer 1	Signature	Date
______________________	____________	______________
Reviewer 2	Signature	Date

Finally, approval and acceptance of the thesis is contingent upon the submission of its final copy to the Office of Postgraduate Studies (OPGS) through the Department Graduate Council (DGC) and School Graduate Committee (SGC).

______________________	____________	______________
Department Head	Signature	Date
______________________	____________	______________
School Dean	Signature	Date
______________________	____________	______________
Office of Postgraduate Studies, Dean	Signature	Date

Acknowledgments

First, I give all glory and honor to the supreme God, the source of all wisdom, knowledge, and understanding. I am thankful to my advisor Dr. Aschalew Tadesse for his constructive comments, encouragement, and assistance in accomplishing this research thesis. My acknowledgment is also extended to Adama Science and Technology University and the department of Applied Chemistry for giving me this chance to endure my academic career.

Table of Contents

Contents pages

List of Tables

List of Figures

List of Abbreviations and Acronyms

AOPs	Advanced oxidation process
CB	Conduction band
DW	Distilled water
FTIR	Fourier-transform infrared spectrometer
LIBs	Lithium-ion batteries
MB	Methylene blue
MNPs	Metallic nanoparticles
MONs	Metal oxide nanostructures
NCs	Nanocomposites
NMs	Nanomaterials
NPs	Nanoparticles
NSs	Nanostructures
PL	Photoluminescence
TGA	Thermogravimetric analysis
TTIP	Titanium tetra-Isopropoxide
VB	Valence band
UV	Ultraviolet
UV-Vis-DRS	UV–Vis diffuse reflectance spectroscopy
XRD	X-ray diffraction

Abstract

This research focuses on the photocatalytic properties of synthesized titanium dioxide and copper oxide nanocomposites (TiO_2/CuO NCs). The synthesis of these TiO_2/CuO NCs was conducted using a sustainable and environmentally friendly green method that involves the utilization of a leaf extract from an Ethiopian endemic plant known as Rosa Abyssinia. This green plant-templated approach embraces the advantages of utilizing readily available natural resources, underscoring the importance of green chemistry in contemporary research. To evaluate the structural and optical characteristics of the synthesized nanomaterials, a series of characterization techniques were employed. These included X-ray diffraction (XRD), which provided insights into the crystal structure and phase purity of the synthesized materials; UV–visible diffuse reflectance spectroscopy (UV-Vis-DRS), which was used to assess the light absorption properties; Fourier transform infrared (FT-IR) spectroscopy, which helped in identifying the functional groups present; and photoluminescence (PL) measurements, which offered information about electronic transitions within the materials. From UV-Vis-DRS analysis the estimated energy band gaps were found to be 2.31 eV for theTiO_2/CuO(2:1) composition, 2.65 eV for TiO_2/CuO(1:1) , and 2.75 eV for TiO_2/CuO (1:2). The FTIR analysis also revealed the presence of TiO_2 *and CuO in the the green synthesized nanocomposites*. *The PL study showed that* TiO_2/CuO (1:1). *The photocatalytic activity of the synthesized nanomaterials was rigorously investigated using methylene blue (MB) dye as a model pollutant. Among the various compositions studied, the TiO_2/CuO nanocomposite in a 1:1 ratio exhibited the most promising photocatalytic performance for the degradation of methylene blue under light irradiation. Several parameters were scrutinized, including the pH of the dye solution, the amount of catalyst used, and the initial concentration of the dye. The results indicated that optimal degradation efficiency was achieved at a pH level of 10, a catalyst loading of 20 mg, and an initial dye concentration of 15 ppm. These findings underscore the potential of using synthesized TiO_2/CuO NCs as efficient photocatalysts for the degradation of organic pollutants, contributing to the advancement of sustainable water treatment technologies.*

***Keywords*:** TiO_2/CuO NCs, photocatalytic degradation, Rosa abyssinica, and methylene blue.

1 Introduction

1.1 Background of the study

The most essential element for life, water, makes up much of the globe. The existence of water is essential for every life on Earth. It makes up 71% of the surface of the planet. The physical characteristics of water include colorless, tasteless, odorless, and clear (Sronsri et al., 2021).Over the last few decades, due to population growth and rapid industrialization, ubiquitous contamination includes organic pollutants, heavy metals, inorganic compounds, and many other complex compounds have been detected in surface, ground, sewage and drinking water resources (Gómez-Pastora et al., 2017). According to the United Nations' World Water Development Report (Boretti & Rosa, 2019), changes in the water cycle will also pose risks to energy production, food security, human health, economic development and poverty reduction, seriously jeopardizing the achievement of sustainable development goals. Therefore, it is essential to develop advanced, environmentally friendly, low-cost and high-efficiency reclamation of wastewater (Zazouli & Kalankesh, 2017).

Nanotechnology is a branch of science that concerns the creation, manipulation, and control of nanoscale materials known as nanomaterials. Nanomaterials are materials with at least one dimension less than 100 nm in length and differ from their bulk counterparts in terms of optical, electrical, and catalytic characteristics (Feiona et al., 2021; Jalab et al., 2021). Based on their physicochemical properties, these materials have a wide range of applications in domains such as energy conversion and storage (Anigol et al., 2017); medicine, and pollution remediation. The chemical, physical, electrical, and optical properties of nanomaterials are all influenced by particle size, shape, and surface morphology (Annu & Ahmed, 2018).

Nanoparticles (NPs) are zero-dimensional particles with all three dimensions in the 1 to 100 nm size range. NPs can be used as a medium of transportation for drug delivery in cancer treatment due to their high bioavailability, efficiency, and improved permeability (Osonga et al., 2020). Nanostructures (NSs) are potentially applied in water and air pollution reduction, energy production, and as antibacterial and anti-viral agents. Nowadays, metal oxide nanostructures (MONSs) get more attention due to their novel optical, electronic, magnetic, thermal, catalytic, and mechanical properties in comparison with their bulk materials (Shanaj & John, 2016). As a result, MONSs were studied and found to be applicable in catalysis, and medical science including antibacterial, antiviral, and anti-carcinogenic, and for the fabrication of sensor, semi-conductor, and capacitive electrodes (Ismail et al., 2019).

The essence of water in our lives can be understood from the fact that no living thing can survive on earth without water. However, water pollution has become a global concern because of the increased addition of different industrial contaminants to drinking water reservoirs (Javed et al., 2021).

Environmental issues are quickly rising to the top of the global agenda. One of these is the affordability of clean water is becoming more and more connected to environmental and health issues. Pollutants like organic dyes can leak into aquatic habitats, which is one of the unintended effects of many new industries and technology. Synthetic dyes are manufactured by a variety of industries, including leather, textile, printing, cosmetics, and pharmaceuticals. They are a significant cause of water pollution (Alizadeh et al., 2017; Hosseini et al., 2022). The cationic water-soluble dyes crystal violet and methylene blue have low biodegradability. Because of this, these dyes damage natural ecosystems by remaining in the environment for extended periods. Ingestion of organic dyes has been linked to several health problems in humans, including vomiting, irregular heartbeat, excessive perspiration, gastritis, and chest pain, according to numerous research (Martins et al., 2022). Consequently, the elimination of these colors from wastewater is the subject of numerous studies. Various strategies have been investigated to eliminate color from industrial discharges and minimize their environmental impact (Bangari et al., 2022; Lu et al., 2022). These include membrane separation (Khan et al., 2023), reverse osmosis, ultra-filtration (Ramutshatsha-Makhwedzha & Nomngongo, 2022), chemical precipitation (Hassanzadeh et al., 2023), adsorption (Cao et al., 2023), and photocatalytic degradation (Elbadawy et al., 2023). Due to its high efficiency, straightforward, working design, and affordable implementation, photocatalytic is regarded as one of the most popular and promising techniques for removing dyes from contaminated water among the methods mentioned above.

The term photocatalysis is the technique of using photons and a catalyst to absorb light to start and speed up chemical reactions that cause the contaminants to mineralize (Danish et al., 2021). There are different types of metal oxides including titanium oxide, copper oxide, cerium oxide, zinc oxide, zirconium oxide, manganese oxide, and tin oxide that can be used in a photocatalytic process, they are thought to be the best in this class because of their high stability over a wide pH range, higher efficiency, affordability, accessibility, low toxicity, and potent ability to oxidize photo-generated holes (Kumari et al., 2023). However, their capacity for photocatalytic degradation is significantly diminished by the rapid recombination of electrons (e−) and holes (h+) (Pattnaik et al., 2023). This issue can be reduced by making nanocomposites of metal oxides. In nanocomposites, due to the lower energy of the valence band of the p-type semiconductor, electrons in the conduction band of the n-type semiconductor will jump on it through the heterojunction, forming nanocomposites of p-n heterojunction at the interface between the p- and n-type semiconductors. Due to electron-hole recombination, a depletion area will consequently arise at the p–n heterojunction interface (Alshaikh et al., 2021). Nanomaterials are synthesized by different synthesis methods, like physical, chemical, and biological methods. Among those methods, the biological method attracts researchers' interest due to its environmentally friendly low cost, and availability. In this work, TiO_2/CuO nanocomposites were synthesized using Rosa abyssinica leaf extract for the degradation of potentially hazardous methylene blue dye.

Rosa abyssinica is found in upland dry evergreen forests, forest borders, bushlands, and dry grasslands, exclusive to Arabia, Ethiopia, Somalia, and Sudan. It is common in central and northern Eritrea. Its fruits serve as food, medicine (protecting against hookworm), live fences, and decorations. This prickly evergreen shrub or small tree can reach up to 7 m in height, with few slightly curved prickles on the stem. The leaves are compound, leathery, consisting of 3 pairs of narrowly ovate leaflets (1-6 cm) with sharp tips and toothed edges on short stalks winged by leafy stipules. The fragrant flowers are white to pale yellow, typically 3-20 in dense heads, each stalked with rounded to square tips and many stamens. The fruits start green and ripen to orange-red, about 2 cm long, fleshy, and edible (Aloi, 2018; Yohannis et al., 2018). The plant photo is shown in Figure 1 below.

Figure 1. Photo of Rosa abyssinica plant.

1.2 Statement of the problem

An increasing global demand for resources leads to energy crises and environmental pollution. Industrialization contributes to water pollution by releasing organic and inorganic pollutants (Zhang et al., 2019), harming human health and aquatic and terrestrial life (Kumari et al., 2023). Common dyes like methylene blue (MB), Crystal violet (CV), Crystal red (CR), and methylene orange are used by industries such as paper, textile, plastics, printing, food processing, pharmaceuticals, leather, and dye production (Ghazy et al., 2022), often discharging untreated sewage into waterways and soils.

Understanding advanced water treatment and recycling technology is crucial due to the gap between water pollution and the global need for industrial water. While various methods have been employed to eliminate harmful contaminants, many lack complete degradation. Heterogeneous advanced oxidation processes using metal oxides are recommended for their simplicity, efficiency under ambient conditions, cost-effectiveness, environmental safety, and minimal secondary pollutant production. Currently, TiO_2 nanomaterials exhibit significant properties across various fields despite challenges like large band gaps and electron-hole recombination. Forming TiO_2-based binary heterojunctions has emerged as a novel approach to enhance the separation of photo-generated electron/hole pairs.

This study used Rosa abyssinica leaf extract to synthesize TiO_2/CuO NCs, the first report of such a synthesis using Rosa abyssinica leaf extract. The photocatalytic activity of the resulting TiO_2/CuO NCs against methylene blue dye was also investigated.

1.3 Objectives of the study

1.3.1 General objective

This work aimed to synthesize titanium dioxide-copper oxide nanocomposites (TiO_2/CuO NCs) using a green synthesis method with Rosa abyssinica leaf and to characterize and evaluate their photocatalytic performance.

1.3.2 Specific objectives

The specific objectives of the present work were:

- ❖ To prepare an extract from *Rosa abyssinica leaf and to identify the phytochemicals that are found in Rosa abyssinica extract.*
- ❖ To synthesize nanocomposites of TiO_2/CuO by green synthesis method using *Rosa abyssinica leaf extracts*.
- ❖ To characterize synthesized composites' size, morphology, and crystal structure using TGA, XRD, FTIR, and UV-Vis.
- ❖ To evaluate the photocatalytic performance of the TiO_2/CuO NCs against MB dye.

1.4 Significance of the Study

Issues about the cleanup of hazardous waste and similar problems have become national and international priorities. According to literary works, the advanced oxidation process (AOP) is an alternate method of removing unwanted contaminants, including colors. TiO_2 has been extensively studied as a heterogeneous photo-catalyst in AOP, where heterogeneous catalysis has been effectively used to degrade several families of hazardous chemicals employing semiconductor materials as a catalyst. Because of their larger specific surface area and smaller particle size, which boost particle surface reactivity, TiO_2 also has appealing antibacterial qualities. Titanium oxide is a biocompatible substance that exhibits photo-oxidizing and photocatalytic effects on both chemical and biological entities. In this study, an n-type TiO_2 is modified with a p-type CuO to enhance its photocatalytic property.

The green method approach is considered a promising route to control the growth, morphology, and properties of the nanocomposites. The aggregation/agglomeration of metal oxide nanocomposites can be avoided by using Rosa Abyssinica leaf extract as a capping agent, which is an eco-friendly, and nontoxic.

1.5 Scope of the study

This work was limited to the synthesis of TiO_2/CuO nanocomposites using the green method with the help of extract Rosa Abyssinica. The prepared material was characterized using XRD, FTIR, UV-Vis-DRS, and PL characterization techniques. The photocatalytic performance of the green synthesized nanocomposites was evaluated using methylene blue as a representative dye. The reusability of nanocomposites was investigated.

2 Literature Review

2.1 Wastewater treatment

Water that has been impacted by residential, commercial, and industrial use is known as wastewater. Contaminants found in wastewater include organic debris, microorganisms, inorganic soluble chemicals, and heavy metals that are poisonous. These contaminants alter the chemical, biological, and physical properties of pure water. Wastewater primarily comes from a variety of businesses, including the agriculture sector (Matheyarasu et al., 2014). Industrial water use is still significantly higher than residential use, but it is far less than that of agriculture. A large amount of wastewater will be produced by companies using a lot of water. Before being released into the environment or recycled, all wastewater must be treated due to environmental contamination and health risks (Selihin & Tay, 2022). Heavy metals, radionuclides, and trace elements are among the hazardous materials found in wastewater, along with big microbes including bacteria, viruses, and protozoa. Additionally, wastewater is a major contributor to waterborne illnesses, which can be fatal and include cholera and typhoid. In 2004, about 1.5 million children under the age of five lost their lives as a result of contaminated water (Baek & An, 2011).

These days, wastewater treatment is crucial due to the harmful effects of pathogens and the risks of wastewater pollution on people, animals, and crops. To prevent pollution of the environment, consideration must be given to wastewater treatment on a personal and governmental level. Physical, chemical, and biological processes can be used to treat wastewater to purify the water of different impurities (Piaskowski et al., 2018).

2.2 Nanotechnology and its Importance

Nanotechnology is the process of controlling matter at the molecular level. Systems based on nanotechnology are quickly spreading throughout society as a means of reducing environmental harm and improving materials. Numerous application areas, including solar power methods, the search for solar energy to meet nuclear energy needs, water propulsion in textile industries, protection from UV rays, quantum computer, hydrogen fuel cell fabrication, light space vehicle design, Nano goods production, biomolecules analysis, smart packaging in the food packaging industry, Nanosensors, and biosensors in the rapid diagnosis of diseases, have all benefited greatly from nanotechnology (Baysal, 2020).

Different studies have shown that positive results have been obtained from nanomaterial treatment of brain tumors since the drugs can be transported to the target site via the blood and brain barrier by using nanoparticles. All the Nanosystems used provide some advantages in pharmaceutics when compared to conventional systems. These advantages are increasing the therapeutic effect by increasing the half-life of the drugs, reducing the side effects of the drugs, monitoring the release and distribution of the drugs, staying in circulation for a long term (Luo et al., 2022), monitoring the treatment efficiency, developing effects without harming other systems and organs, avoiding some drug use problems like drug application at night, forgetting to take or administer drugs, using drugs in short time intervals, etc. Also in other areas such as industry, nanotechnology has high acceptability due to its compatible size (Singh et al., 2004).

In the development of drug delivery applications, Nanocarriers are designed in different pharmaceutical forms including oral, parenteral, pulmonary, nasal, transdermal, or topical formulations (Karatas et al., 2020). Delivery of the drug to the structure where it will activate is one of the main problems of pharmaceutical technology. Drug use is limited due to situations such as low drug solubility, overdose, formation of toxicity, non-specific transfer, short half-life period, etc. Today, many researchers participate in activities of developing new drug delivery systems to minimize the increasing problems of drugs and to turn new developments into clinics (Onoue et al., 2012). In addition to that nanotechnology has other different application areas in health such as Cancer treatment (damage to the rapidly proliferating cells) and wound healing which means a slower release of the nanoparticles than the gel increases the retention time on the skin, treatment of infectious diseases, Diabetes treatment, etc. (Karatas et al., 2020).

2.3 Metal oxide nanomaterials

Metal oxide nanostructures have received greater interest in materials research recently because of their unique properties, which include exceptional thermal and electrical conductivity, variable bandgap/band edge locations, high natural abundance, and great chemical stability (Bano et al., 2020). In terms of size or shape-dependent physicochemical and functional qualities, chemical and thermal stability, and a wide range of applications, nanostructured metal oxides outperform their bulk counterparts. Metal oxide-based nanostructures have been extensively researched for use in sensors, catalysis, superconductors, electronics, energy production and storage, medicine, and other medical sectors because of these exceptional qualities and benefits (Kumar et al., 2020; Murthy et al., 2020; Pandit & Sankapal, 2021).

Since the materials utilized in a certain field's practical use must have specified attributes, like a large surface area, outstanding stability, good recoverability, and suitable bandgap/band edge potentials, producing a metal oxide nanostructured single component. Finding material that satisfies every criterion is difficult(Baumgarten et al., 2022; Paydar et al., 2021). To fulfill the conditions of a particular application, numerous alteration techniques have been developed by modifying qualities such as surface, electrical and optical properties, shape, composition, and characteristics, and others using methods including morphology, defect engineering, and doping optimization, the formation of composites, or coupling with substances like carbon or noble metals additional semiconductors and nanostructures (Thakur & Mandal, 2020; Wang et al., 2018).

2.3.1 Titanium oxide (TiO_2)

Due to its non-flammable and non-toxic properties, titanium dioxide (TiO_2) is a solid transition metal oxide that is reasonably abundant and environmentally benign. Once more, TiO_2 exhibits strong thermal stability, and good resistance to corrosion, and oxidation (Roy, 2022). TiO_2 is an excellent semiconducting material. TiO_2 NPs have good electrical, optical, and magnetic properties. TiO_2 NP is extensively used as a photocatalyst, antimicrobial agent, and electrode material for energy storage devices such as lithium-ion batteries, and supercapacitors. TiO_2 naturally occurs in three crystalline forms, these are rutile, anatase, and brookite, with band gaps of 3.0, 3.2, and 2.96 eV, respectively. Anatase and rutile have tetragonal structures with different space groups (Low et al., 2017). The lattice arrangement of anatase makes it the most electrochemically active phase and efficient photocatalyst among all naturally occurring crystalline forms of TiO_2 (Blangetti et al., 2023).

Rutile is the most frequent form, with a tetragonal structure, 6 oxygen atoms per unit cell, and TiO_6 as an octahedron that is slightly deformed. Rutile is the most thermodynamically stable phase of TiO_2, with a low value of Gibbs free energy at atmospheric pressure compared to anatase and brookite. Rutile transforms irreversibly from anatase and brookite to rutile during calcination, beginning at 600 ^{o}C and ending at 900 ^{o}C. Anatase has a tetragonal structure as well, even though the TiO_6 octahedron in the anatase phase is more deformed than in the rutile phase. Anatase is more stable at low temperatures, and rutile and anatase are widely utilized in photocatalysis processes. Because the conductive band of anatase is closer to the negative position than that of rutile, it is more photoactive. This increases the reducing power. Furthermore, the Fermi level is somewhat higher, with strong electron mobility, low density, and lower surface energy, all of which contribute to the application of anatase (Aslam et al., 2020; Rao et al., 2016). The characteristics of TiO_2 crystals are listed in Table 1.

Table 1. Some Main Properties of TiO_2 Crystal.

Properties	Brookite	Anatase	Rutile
Stability	metastable	Metastable	Stable
Structure	Orthorhombic	Tetragonal	Tetragonal
Cell volume	137.19 $Å^3$	140.68 $Å^3$	140.41 $Å^3$
Lattice constant(Å)	a= 4.9022 Å	a= 4.979 Å	a= 4.9732 Å
	b= 9.459 Å	b= 9.5613 Å	b= 9.5425 Å
	C=2.958 Å	c= 2.9551 Å	C= 2.9586 Å
Photocatalytic activity	Medium	High	Low
Melting point (^{o}C)	Transformation to rutile	Transformation to rutile	1825

2.3.2 Copper oxide nanoparticle (CuO)

Studies on transition metal oxides (MOs) have focused a lot of attention on cupric oxide (CuO) due to its intriguing characteristics as a p-type semiconductor with a tight band gap (1.2 eV in bulk) and as the building block for several high-temperature superconductors and enormous magneto resistance materials (Anjum et al., 2023; Zhang et al., 2014). Large surface area CuO nanostructures with possible side effects have better physical and chemical characteristics than their micro or bulk counterparts. Because these nanostructures offer promising uses across a range of industries, they have been thoroughly studied. Science of CuO nanostructures' great theoretical capacity, safety, and environmental friendliness, they are also being evaluated as electrode materials for the next generation of rechargeable lithium-ion batteries (LIBs) (Gebremedhin et al., 2023; Song et al., 2021). Their high carrier concentration, low thermal emittance, strong solar absorption, and generally acceptable electrical qualities make them suitable materials for the creation of solar cells. Gas sensors, bio-sensors, Nanofluid, photodetectors, energetic materials (EMs), field emissions, supercapacitors, removal of inorganic pollutants, photocatalysis, and magnetic storage media are just a few of the numerous additional applications that CuO nanostructures are widely used in (Anand et al., 2023; Meena et al., 2023; Sayyed et al., 2023). Recent studies have demonstrated that nanoscale CuO can prepare various organic-inorganic nanocomposites with high thermal, electrical, mechanical, and high-temperature durability (Sayyed et al., 2023).

2.4 Photocatalysis

The removal of contaminants is the main goal of several wastewater treatment techniques. These consist of advanced oxidation techniques such as photocatalysis, biological processes, adsorption processes, electrochemical oxidation, and physicochemical procedures (Rezaei et al., 2023; Salem et al., 2023). When it comes to removing organic contaminants from water, photocatalytic degradation is the most promising approach due to its ease of use, speed, cleanliness, and affordability when compared to other methods that require large running expenses and take a long time (Rezaei et al., 2023). The application of photon energy to start a specific reaction process is known as photocatalysis. As a result of their ability to eliminate various organic contaminants present in water through a sequence of redox processes, semiconductor materials have gained more attention in the photocatalysis community. The stimulation of electrons from the valence band to the conduction band brought on by the absorption of a photon at the right wavelength is linked to semiconductors' capacity for photocatalysis (Yitagesu et al., 2023).

2.4.1 Photocatalytic application of TiO_2/CuO NCs

An interface between two layers or regions of different crystalline semiconductors is known as a heterojunction. As was mentioned in a previous section, titanium dioxide is used intensively for photocatalysis applications. However, the photocatalytic activity of titanium dioxide is constrained by two criteria. These elements include the quick recombination of positive holes and electrons as well as the large band gap. By separating positive holes and electrons and closing the band gap, the heterojunction of titanium dioxide with other semiconductor metal oxides is another attempt to enhance photocatalytic activity. The creation of titanium dioxide heterojunctions or composites with other semiconductors has drawn a lot of interest (Kubiak et al., 2020). The development of heterojunction increases catalytic efficiency by shifting titanium dioxide's absorption capability to the visible wavelength side. Various semiconductor metal oxides can be utilized to create heterojunctions. One semiconductor that might be utilized to create a heterojunction of titanium dioxide is zinc oxide (ZnO). Zinc oxide has strong catalytic activity and a band gap resembling that of titanium dioxide. It is therefore anticipated that under visible light irradiation, the TiO_2-CuO heterojunction will demonstrate strong photocatalytic performance. The fabrication of CuO-TiO_2 heterojunction as an effective photocatalyst for the photodegradation of methyl orange has been reported (Janczarek & Kowalska, 2017).

2.4.2 Photocatalysis mechanism

Exciton or electron/hole (e-/h+) pairs emerge when the photocatalyst absorbs the necessary energy of light, with holes in the valence band and electrons in the conduction band, as illustrated in Figure 2 and Figure 3. Each of the charge carriers may go in different directions depending on the surroundings and band edge positions of the adsorbed species' redox potential. In the valance band, holes cause oxidation, whereas in the conduction band, electrons cause a reduction. Alternatively, both holes and electrons may combine again. Reactive oxygen species (ROS) as superoxide anion radicals (O_2•−), hydroxyl radicals (•OH), singlet oxygen species (•O_2), and peroxide molecules (H_2O_2) are therefore produced by the charge carriers. The redox reactions mentioned above are listed below in Equations 1-8.

$$\mathbf{semiconductor + hv \rightarrow Semiconductor(h_{VB}^{+} + e_{CB}^{-})} \quad (1)$$

$$\mathbf{e_{CB}^{-} + O_2 \rightarrow O_2^{\bullet -}} \quad (2)$$

$$\mathbf{O_2^{\bullet -} + H^{+} \rightarrow HO_2^{\bullet}} \quad (3)$$

$$\mathbf{2HO_2^{\bullet} \rightarrow H_2O_2 + O_2} \quad (4)$$

$$\mathbf{2HO_2^{\bullet} \rightarrow H_2O_2 + O_2^{\bullet -} \rightarrow OH^{\bullet} + O_2 + OH^{-}} \quad (5)$$

$$\mathbf{h_{VB}^{+} + OH^{-} \rightarrow OH^{\bullet}} \quad (6)$$

$$\mathbf{h_{VB}^{+} + H_2O \rightarrow OH^{\bullet} + H^{+}} \quad (7)$$

$$\mathbf{OH^{\bullet} + MB \rightarrow \mathit{CO_2 + H_2O + Minerals}} \quad (8)$$

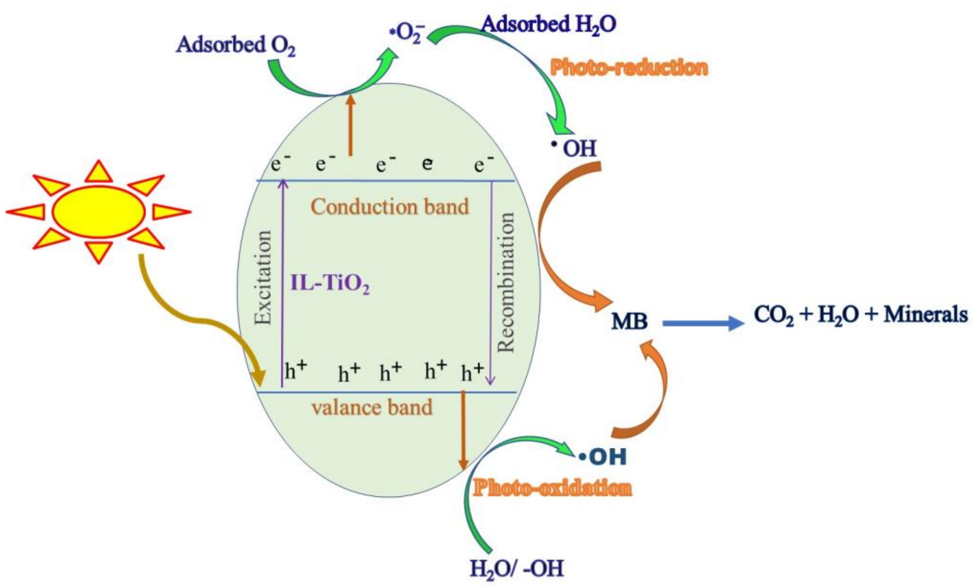

Figure 2. The proposed photodegradation mechanism of methylene blue (Yitagesu et al., 2023).

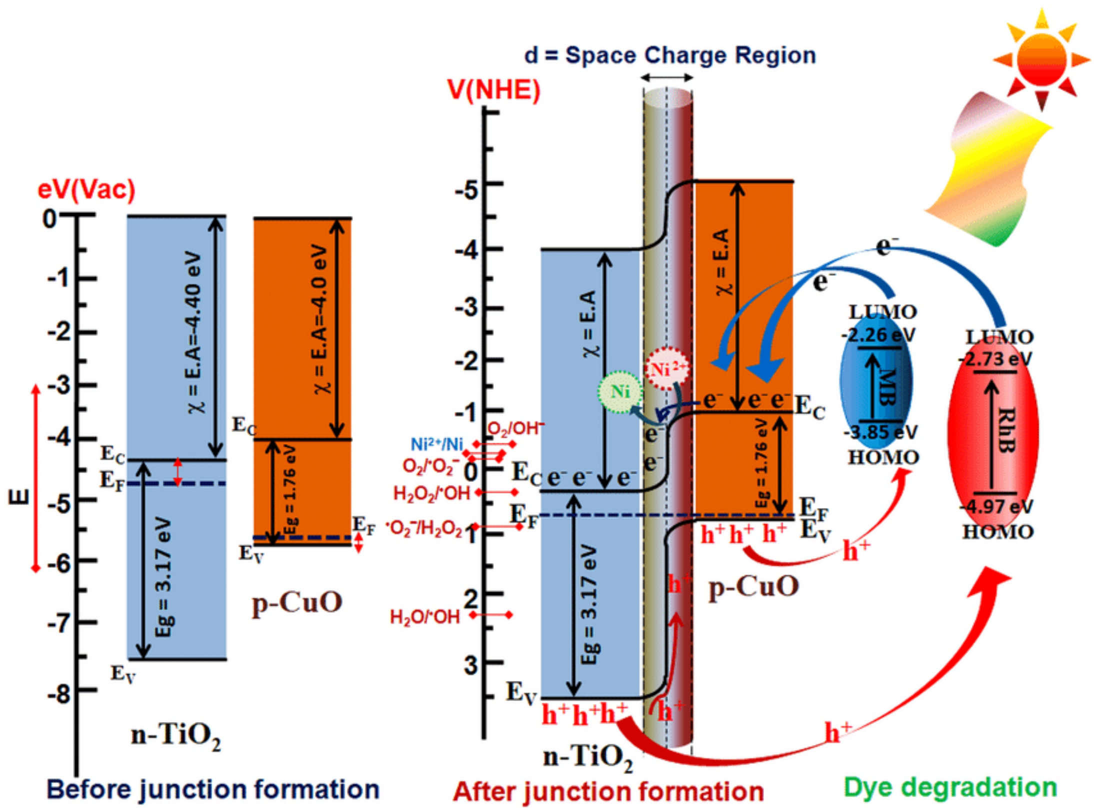

Figure 3. Energy band diagram for TiO_2/CuO heterojunction, before and after contact, with the photocatalytic mechanism for the degradation of organic dyes and Ni^{2+} ion reduction (Ahamed et al., 2020).

2.5 Synthesis methods of nanomaterials

Basic synthesis methods for nanomaterials include physical, chemical, and biological/green approaches. These synthesis methods can be further divided into bottom-up and top-down approaches. Nanoparticles are initially obtained at the atomic level and then incorporated into the appropriate material via the bottom-up technique. This comprises the creation of NPs from colloidal dispersion and powders from the sol-gel technique, followed by integration (Saleh, 2020). The build-up of material from atoms to clusters to nanoparticles is known as the bottom-up or constructive process. The most prevalent bottom-up processes for nanoparticle generation are sol-gel, spinning, chemical vapor deposition (CVD), pyrolysis, and biosynthesis (Ealia & Saravanakumar, 2017; Rana et al., 2024). Some of the synthesis methods are shown in Figure 4 (Álvarez-Chimal & Arenas-Alatorre, 2023).

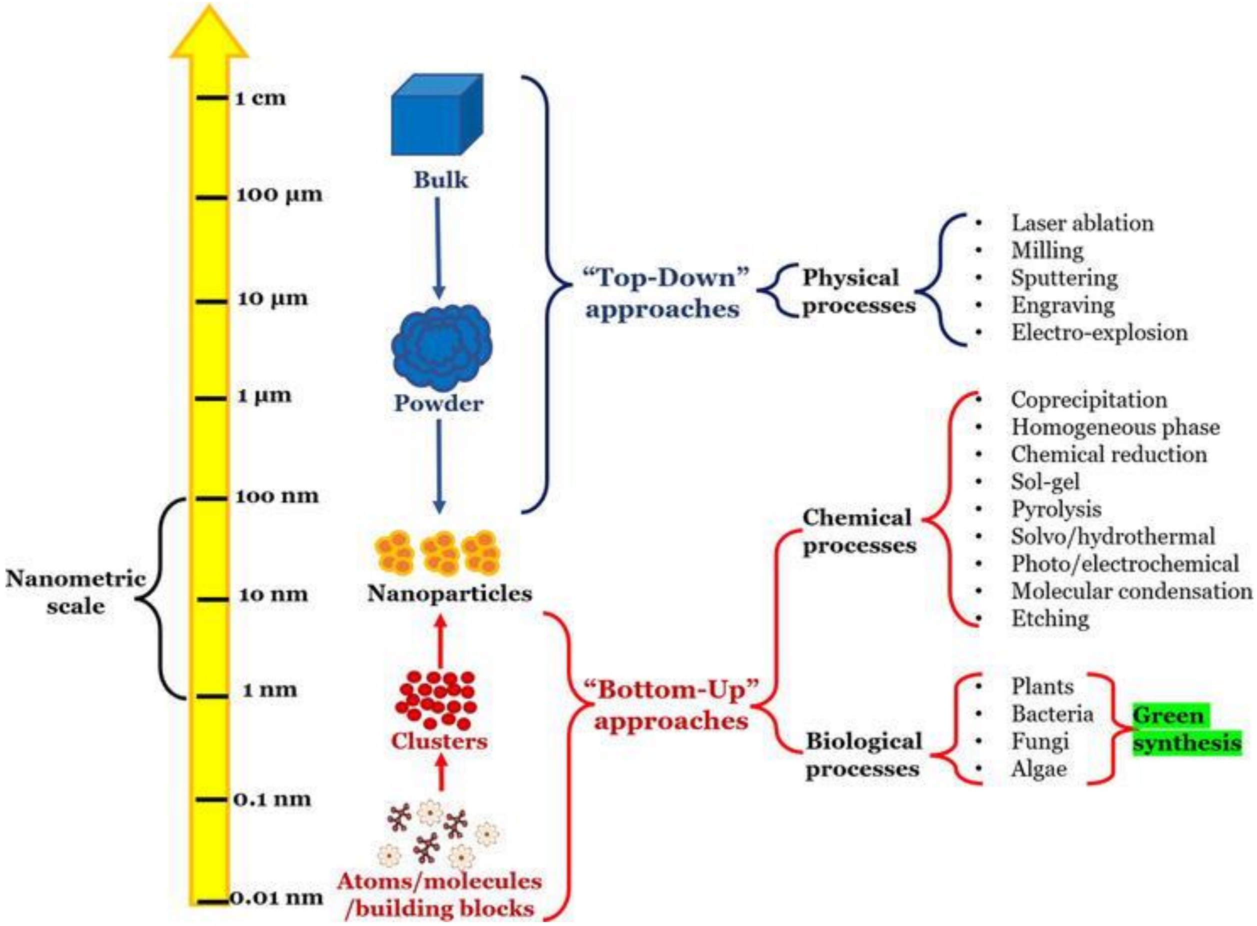

Figure 4. Different nanoparticle synthesis approaches and methods (Álvarez-Chimal & Arenas-Alatorre, 2023).

2.5.1 Microwave heating

Irradiation with microwaves (MW) is a quick and easy way to produce energy for chemical reactions. Microwave technology is a powerful energy source capable of completing chemical changes in minutes rather than hours or days of high-temperature heating. Microwaves are electromagnetic waves with frequencies ranging from 0.3 to 300 GHz and wavelengths ranging from 1 mm to 1 m that are used in microwave-assisted procedures. The two major methods of microwave heating are dipolar polarization and ionic conduction (Nyamukamba et al., 2018). Microwave heating may have various advantages over traditional heating, including faster reaction times, higher heating rates, and better product uniformity (Machut et al., 2020). Table 1 shows examples of nanomaterials synthesized through the microwave method.

Table 2. Nanomaterials synthesized by microwave and their applications.

Nanomaterials	application	Reference
TiO_2/CuO	photocatalysis	(Kubiak et al., 2020)
TiO_2/CuO	photocatalysis	(Kannan et al., 2021)=
TiO_2/Au	photocatalysis	(May-Masnou et al., 2018)
CuO/CoO	photocatalysis	(Gouasmia et al., 2022)

2.5.2 Sol-Gel Method

The sol-gel method of material synthesis is a straightforward, low-cost, and low-temperature procedure. The early development of a gel ensures great homogeneity and eliminates the requirement for atomic diffusion during solid-state calculations. Furthermore, metal alkoxides are frequently used as precursors, as many of them are liquids or volatile solids that may be easily filtered, resulting in exceptionally pure oxide precursors. This component is crucial in the production of electroceramics. The comparatively high costs of metal alkoxides, on the other hand, may be prohibitive for some applications, and the release of considerable volumes of alcohol during the calcination stage necessitates specific safety precautions. After forming a solution containing the suitable precursors, hydrolysis and condensation are used to convert the solution into homogenous oxide (gel). The oxide product is obtained by drying the gel and then calcining it. Alkoxides are usually combined in alcohol to make multi-component oxides. Acetates and other components for which no alkoxides are available are introduced as salts. The temperature, pH, and concentration of alkoxides, as well as the addition of water and alcohol, are all controlled during the hydrolysis process (Srivastava, 2012). Table 4 shows some examples of nanomaterials synthesized by sol-gel methods.

Table 3. Nanomaterials synthesized by sol-gel methods.

Nanomaterial	application	References
TiO_2/CuO	photocatalysis	(Khoroshko et al., 2023)
TiO_2/CuO	photocatalysis	(Chi & Wang, 2022)
TiO_2/CuO	photocatalysis	(YILDIRIM et al., 2010)
TiO_2/CuO	photocatalysis	(Muzakki et al., 2016)
TiO_2/CuO	photocatalysis	(Celik et al., 2006)
TiO_2/CuO	Photocatalysis	(Roy, 2022)

2.5.3 Green synthesis

The use of physical and chemical processes to make nanoparticles produces hazardous byproducts that are harmful to the environment. As a result, the green synthesis approach is thought to be a promising alternative for producing biocompatible and stable nanoparticles. The bottom-up technique is used in biologically based nanoparticle production (Patra & Baek, 2014). Green synthesis methods are needed to avoid the formation of toxic byproducts by developing dependable, long-lasting, and environmentally friendly synthesis procedures. The synthesis of nanoparticles by fungi, bacteria, algae, and plants is a common green synthesis approach (Singh et al., 2018). Plant-derived nanoparticles are more long-lasting, cost-effective, and quite innovative. Plant extracts have the advantage of being dual-purpose, working as both reducing and stabilizing agents to aid in the creation of nanoparticles (El Shafey, 2020; Gnanasangeetha & Suresh, 2020). Figure 5 shows the general mechanism of green synthesis. Examples of nanomaterials synthesized by green methods using plant extract are listed in Table 3.

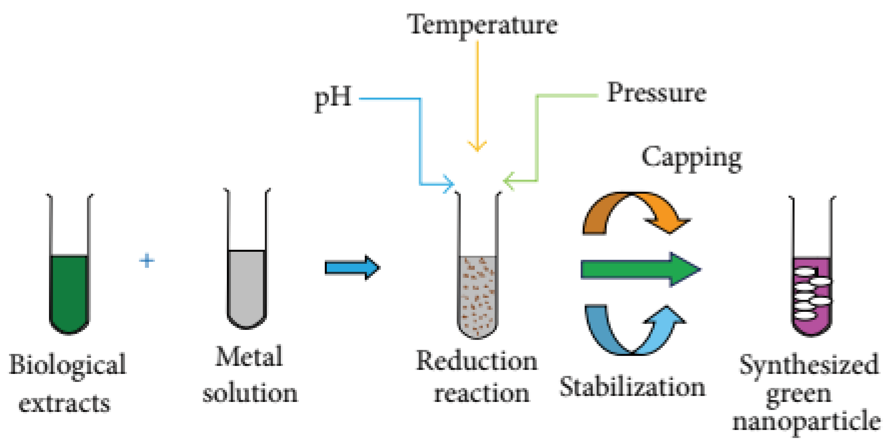

Figure 5. Biological synthesis of nanoparticles using green technology (Patra & Baek, 2014).

Table 4. Examples of green synthesized nanomaterials.

Plant	nanomaterial	Application	References
Rubus ellipticus	TiO_2/CuO	photocatalysis	(Bisht et al., 2023)
C. benghalensis	TiO_2/CuO	photocatalysis	(Bopape et al., 2023)
A. carambola	TiO_2/CuO	photocatalysis	(Etape et al., 2017)
Moringa Oleifera	TiO_2/CuO	photocatalysis	(Solano et al., 2023)
Eichhornia crassipes	TiO_2/CuO	photocatalysis	(Lu et al., 2019)

3 Materials and methods

3.1 Apparatus and instruments

Apparatuses used during this research work were: Fourier-transform infrared spectrometer (FTIR), x-ray diffractometer (XRD), Ultraviolet-visible spectrophotometer (UV-Vis), centrifuge, digital electronic balance, furnace, refrigerator, ultrasonic bath/sonicator, different size of beakers, test tubes, magnetic stirrer, thermometer, Whatman filter paper, mortar and pestle, cylindrical glass, pH meter, micro grinding machine, hot plate, micropipettes, spatulas, Erlenmeyer flasks, volumetric flasks, crucible, and aluminum foils.

3.2 Chemicals and reagents

The chemicals and reagents used in this work were distilled water, Titanium tetra isopropoxide (27%), ethanol (99%), isopropanol (99%), hydrochloric acid (37%), NaOH, and copper nitrate. All reagents used in this work were analytical grades.

3.3 Sample Collection and Extract Preparation

The fresh plants' part of *Rosa abyssinica* leaf was collected from the forest of Amhara regional state, Awi zone, Gashena wereda. The plant part used in this study was extracted from the *Rosa Abyssinia leaf* washed with distilled water and dried. After crushing into fine powder using a mortar and pestle, the extract was prepared using distilled water. Then the mixture was stirred and heated at 60 for 2 hrs. The solution was filtered using Whatman filter paper. The extracted part was stored at 4 ^{0}C for further use (Chatterjee, 2018; El-Ghamri et al., 2015; García-Salinas & Ariza, 2019).

3.4 Phytochemical Analysis

3.4.1 Test for Alkaloid

1 mL of the *Rosa abyssinica* leaf extract filtrate was treated with a few drops of Wagner reagent, and a yellow color formation was observed (Bakatula et al., 2018).

3.4.2 Test for Flavonoid

The *Rosa abyssinica* leaf extract was mixed with a few fragments of magnesium ribbon, and concentrated HCl was added dropwise. The appearance of pink scarlet has been looked at to indicate the presence and absence of flavonoids (Saha et al., 2020).

3.4.3 Test for Phenol

1 mL of the *Rosa abyssinica* leaf extract filtrate was taken in a test tube, and 1 to 2 drops of iron III chlorides ($FeCl_3$) were added. The color change of the mixture was observed after a few minutes (Oloya et al., 2022).

3.4.4 Test for Saponins

The filtrate of plant extract (1 mL) was taken in a test tube and diluted with 5 mL of distilled water. It was shaken by hand for 15 minutes. A foam layer was observed on the top of the test tube. This foam layer indicated the presence of saponins (Agidew, 2022).

3.4.5 Test for Steroids

The plant extract filtrate (1 mL) was taken in a test tube and dissolved in chloroform (1 mL). Then the sides added 1 mL of acetic anhydride and 2 drops of concentrated sulfuric acid to the test tube. The upper layer in the test tube turned red, indicating the presence of steroids (Dubale et al., 2023).

3.4.6 Tannins Test

The plant extract filtrate (2 mL) was taken, and then a few drops of 10% ferric chloride solution were added to the filtrate. The blue-green color appearance indicates the presence of tannins in the sample (Oloya et al., 2022).

3.4.7 Test for proteins

In a dry test tube, 2mL extract was taken and then HNO_3 solution was added drop wisely. The formation of yellow color shows the presence of proteins (Saha et al., 2020).

3.4.8 Terpenoids Test

The plant extract filtrate (1 mL) was taken in a test tube and dissolved in chloroform (1 mL). The concentrated sulfuric acid (2 drops) was added to the test tube and shaken. The lower yellow color indicates the presence of terpenoids (Dubale et al., 2023).

3.5 Green synthesis of TiO_2/CuO nanocomposites

The TIO_2/CuO nanocomposites were synthesized using the facile green synthesis route using Rosa abyssinica leaf extract which acts as a reducing/capping agent. 20 mL of Titanium tetra isopropoxide (TTIP) was added to the beaker containing absolute ethanol and distilled water in a ratio of 1:1 with a volume of 50 ml. The solution 0.5 molars of copper nitrate solutions of 10, 20, and 40 ml were taken separately, to make the ratio of CuO and TiO_2 in such a way that 2:1, 1:1, and 1:2 by precursor volume. The CuO precursor solution was slowly poured into the titanium solution while stirring magnetically. Then 50 mL extract of Rosa abyssinica was poured to the mixture step wisely. The solution was stirred at room temperature until the color change was observed which confirms the formation of titanium dioxide-copper oxide nanocomposites. The synthesized nanocomposite solutions were separated by filtering using the Whatman No1 filter paper. The isolated nanocomposites were dried in an oven at 100 ^{0}C overnight and calcined based on TGA stability information (Ahmad et al., 2020; Aravind et al., 2021; Muniz et al., 2011). Then the synthesized Nanomaterials were characterized by XRD, FTIR, and DRS characterization techniques.

3.6 Characterization of the as-synthesized TiO_2/CuO nanocomposites

Several characterization approaches were used to examine the properties of the biosynthesized nanomaterials. The XRD study was performed on a Shimadzu 7000 X-ray diffractometer (Japan) equipped with Cu Kα1 radiation source (λ = 1.5406 Å) with an accelerating voltage of 40 kV and a source current of 30 mA at a scanning rate of 4° min^{-1} in 2θ range of 10 ° to 80 °. The UV-Vis defused reflectance spectrophotometer (JASCO V-750 UV-Vis) has been utilized to measure the UV-Vis diffused reflectance spectra. FTIR spectra were obtained using an FTIR-6600 spectrophotometer (JACO International Co., Ltd., Tokyo, Japan) between 4000 and 400 cm^{-1}. UV-Vis spectrophotometer was used to study the degradation of the MB dye.

3.7 Photocatalytic activity

The degradation of an aqueous solution of MB with varying concentrations of MB was used to assess the photocatalytic activity of the synthesized NCs. The reactions took place in a mechanical stirring photo reactor that was illuminated by 150 W halogen lamps. 20

mg of synthesized nanomaterials were introduced to a 100 mL aqueous solution of MB dye while it was being constantly stirred to effectively degrade the dye. Before irradiation, the solution was continually shaken in the dark for approximately 35 minutes to establish an equilibrium for adsorption-desorption between the photocatalysts and MB dye. Then, the light source was positioned on top of the solutions and was irradiated under continuous stirring. The decomposed dye sample was periodically withdrawn every 10 min and subjected to centrifugation to separate the nanomaterials from the dye solution. The absorption spectra of decomposed dye were collected using a UV–visible spectrophotometer (UV-3600 Shimadzu Co., Japan). Finally, the photocatalytic degradation efficiencies of the samples were calculated using the following equation (Equation 9) (Cahino et al., 2019).

$$Degradation\ rate = \frac{C_o - C_t}{C_o} \times 100 \tag{9}$$

Here C_0 is the initial dye concentration and C_t is the concentration at time, t. All concentration values were obtained by the wavelength of maximum absorption (λ_{max}= 664 nm) for MB in the absorption spectrum.

The effects of catalyst dosage (10, 20, and 30 mg), pH (4, 7, and 10), and concentration of MB (10, 15, and 20 ppm) were investigated by using TiO_2/CuO NCs catalyst for degradation of MB. According to the first-order kinetics reaction, rate constant k (min^{-1}) was determined by using the following Equation 10 (Alkaykh et al., 2020).

$$ln\left(\frac{C_o}{C_t}\right) = kt \tag{10}$$

Where C_0 is the initial concentration of the MB, C_t is the final concentration after visible light irradiation and k is the rate constant.

3.8 Reusability test

The recyclability tests were done for synthesized nanocomposites after being used in the photocatalytic degradation of MB. After the first photocatalysis degradation, the solution was centrifuged three times with distilled water. Then the washed synthesized nanocomposites will be dried at 70 ^{0}C and reused. This procedure was repeated for three consecutive additional cycles' of photocatalysis using fresh MB dye.

4 Results and discussion

4.1 Phytochemical Screening Result

The *Rosa abyssinica* leaf extract was presented with notable positive phytochemical results (Table 5), which were evidenced with remarkable color changes. Flavonoids, saponins, alkaloids and phenols were the abundant classes of compounds in the majority of the screened plant extract. Only the protein test showed a negative phytochemical screening test indicating its absence.

Table 5. Phytochemical test response of *Rosa abyssinica* leaf extract.

Phytochemicals	Response to the test
Alkaloids	+
Flavonoids	+
Phenols	+
Saponnins	+
Steroids	+
tannins	-
Proteins	-
Terpenoids	+

4.2 XRD Analysis

The crystalline structure and phase purity of the samples were characterized using X-ray diffraction (XRD) analysis. The results from the XRD patterns corresponding to the biosynthesized titanium dioxide/copper oxide nanocomposites (TiO_2/CuO NCs) are illustrated in Figure 6. Specifically, the XRD analysis revealed the presence of titanium dioxide characterized by distinct diffraction peaks at specific 2θ angles, notably 25.28 ^{o} corresponding to the (101) plane, 36.85 ^{o} for the (103) plane, 37.82 ^{o} for the (004) plane, 48.14 ^{o} associated with the (200) plane, 53.75 ^{o} for the (105) plane, 55.15 ^{o} relating to the (211) plane, and further peaks at 62.79 ^{o} (204), 68.74 ^{o} (116), 70.35 ^{o} (220), and 75.13 ^{o} (215). These peaks are indicative of the anatase phase of titanium dioxide and align with the reference data cataloged in the Joint Committee on Powder Diffraction Standards (JCPDS) file number 21-1272 (Gou & Guo, 2019) Additionally, the analysis presented prominent diffraction peaks for copper oxide within the range of 2θ values that include 32.52 ° for the (110) plane, 35.65 ° for the (-111) plane, and 38.84 ° for the (111) plane. These findings confirm the successful formation of copper oxide, consistent with the standard JCPDS reference number 48-1548 (Ramírez et al., 2020). The clear presence of notable diffraction peaks from both the titanium dioxide and copper oxide components conclusively demonstrates the formation of the TiO_2/CuO nanocomposite structure, highlighting the effective biosynthesis process employed.

The average crystallite size of the biosynthesized NCs was estimated from the major intense peaks by using the Scherer formula, Equation 12.

$$D = \frac{K\lambda}{\beta\cos\theta} \tag{12}$$

Where K is Scherer's constant, which is 0.9, λ is the wavelength of the X-ray radiation, which is 0.15406 nm, β is peak width at half maximum, and θ is Bragg's angle. The calculated average crystallite sizes of TiO_2/CuO (1: 1), TiO_2/CuO (1:2) and TiO_2 (2: 1) biosynthesized by Rosa abyssinica leaf extract were 12.5, 14, and 17nm, respectively.

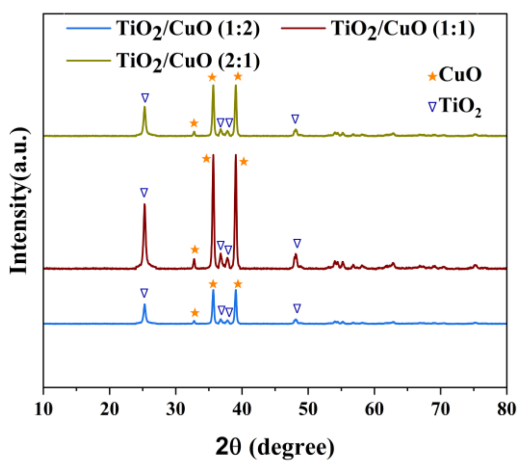

Figure 6. XRD patterns of biosynthesized TiO_2/CuO (1: 1), TiO_2/CuO (1:2) and TiO_2 (2: 1) *NCs.*

4.3 UV-Vis DRS analysis

The optical properties of synthesized samples were analyzed via UV-Vis DRS, and their Tauc plots were drawn using the standard procedure and mathematical calculations (Figure

7). The band gap energy of the as-synthesized NPs' was calculated using the Tauc equation 13 (Tauc et al., 1966).

$$(F(R) \cdot h\upsilon)^{n} = A \cdot (h\upsilon - E_{g}) \quad (13)$$

where F(R) is the percentage of reflected light, h is Planck's constant, ν is incident light frequency, E_g is the bandgap energy, A is a proportionality constant, and n is the power index that is related to the characteristics transition in a semiconductor (n = 2). The optical bandgap energy of the NPs was estimated by plotting the $(F(R) \cdot hv)^{n}$ versus the photon energy (hυ) and extrapolating the linear region of the curve to the energy axis.

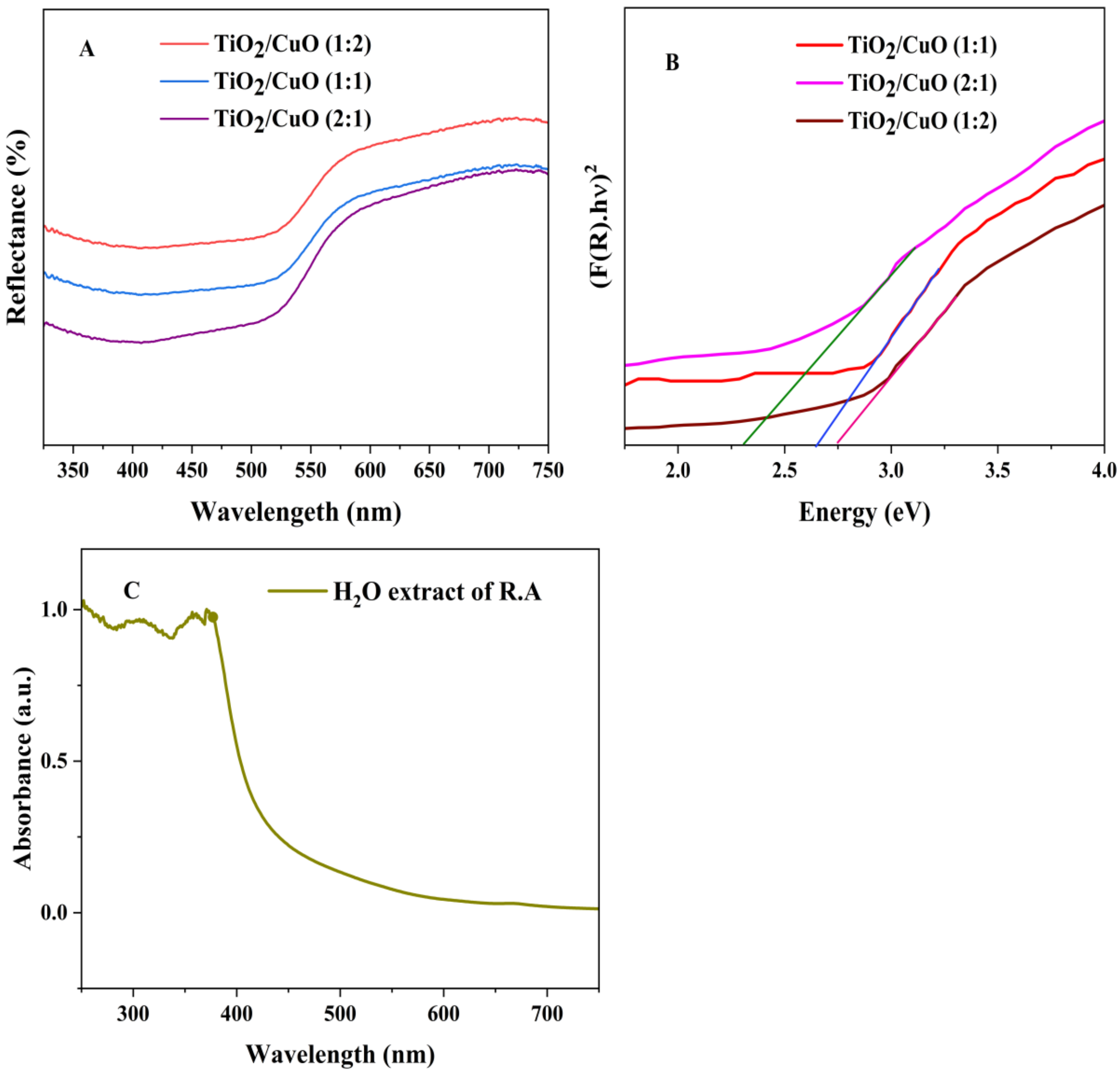

Figure 7. UV–Vis DRS spectra of TiO_2/CuO NCs (A), Tauc plots for bandgap energy estimation (B), and UV-Vis spectra of R.A extract (C).

Figure 7 shows the energy band gap of TiO_2/CuO NCs obtained from Tauc plots. The estimated energy band gaps of TiO_2/CuO (2: 1) TiO_2/CuO (1: 1), and TiO_2/CuO (1:2) biosynthesized by Rosa abyssinica leaf extract were 2.31, 2.65, and 2.75 eV, respectively. The energy was found to be decreased with a decreasing ratio of Titanium oxide precursor. Figure 7C shows the UV-Vis absorbance spectra of plant extract which indicates the presence of polyphenols in the extract (Halake & Lee, 2017).

4.4 FTIR Analysis

The FTIR spectra of TiO_2/CuO NCs are shown in Figure 8. The absorption peaks at about 3408 and 1629 cm $^{-1}$ are related to the stretching vibration of surface hydroxyl groups and the H-O-H bending vibration of adsorbed water molecules, respectively (Adyani & Ghorbani, 2018). The weak absorption band at around 2337 cm $^{-1}$, can be related to the absorption of CO_2 from the atmosphere. The peaks at 2,915 and 2,850 cm $^{-1}$ are assigned to C–H stretching vibrations of alkane groups. Small absorption peaks between 400 and 460 cm $^{-1}$ are attributed to Ti-O-Ti vibrations. Further observation shows that the peaks corresponding to the vibration of 450-680 were ascribed to the stretching modes of Cu–O and Cu–O–Cu bridging (Sethy et al., 2020).

The Fourier Transform Infrared (FTIR) spectra of the titanium dioxide/copper oxide nanocomposites (TiO_2/CuO NCs) are presented in Figure 8. Analysis of the spectra reveals significant absorption peaks, notably at approximately 3408 cm $^{-1}$ and 1629 cm $^{-1}$. These peaks can be attributed to the stretching vibrations associated with surface hydroxyl groups, which play a critical role in the chemical reactivity and interaction of the nanocomposites with environmental factors (Sayed et al., 2024; Shawky et al., 2024). The peak at 1629 cm $^{-1}$ corresponds to the H-O-H bending vibration of water molecules that are adsorbed onto the surface of the TiO_2/CuO NCs, indicating the presence of moisture within the sample, which is essential for understanding its surface chemistry and potential applications (Adyani & Ghorbani, 2018). In addition to these prominent features, a relatively weak absorption band is observed around 2337 cm $^{-1}$. This particular peak is suggestive of the absorption of carbon dioxide (CO_2) from the surrounding atmosphere, pointing to the nanocomposite's possible interactions with prevalent greenhouse gases, a factor that may influence its performance in environmental applications. Furthermore, the spectra exhibit peaks at 2915 cm $^{-1}$ and 2850 cm $^{-1}$, which are attributed to C–H stretching vibrations indicative of alkane groups. These vibrations may arise from organic contaminants or stabilization agents present in the synthesis process, highlighting the complex surface chemistry of the nanocomposites.

The spectrum also shows small absorption peaks in the range of 400 to 460 cm $^{-1}$, which are linked to the Ti-O-Ti vibrations. These vibrations are emblematic of the titanium-oxygen bonding within the crystal structure of TiO_2, reinforcing the structural integrity and stability of the nanocomposite. Further analysis of the spectral data reveals additional peaks corresponding to the range of 450-680 cm $^{-1}$ (Sethy et al., 2020). These peaks are attributed specifically to the stretching modes of Cu–O and Cu–O–Cu bridging, which are significant for understanding the copper oxide component's influence on the overall characteristics of the nanocomposites (Sethy et al., 2020). The presence of these distinct vibrational modes provides valuable insight into the molecular interactions and bonding environments within the TiO_2/CuO NCs, thereby contributing to the knowledge necessary for their potential applications in various fields, including catalysis and environmental remediation. As shown in Figure 8A The FTIR analysis of plant extract also showed that the peak at 3341 cm^{-1} is related to the presence of O-H stretching. The band around 2923 cm^{-1} is corresponding to C-H stretching. The absorption peak at 1637 cm^{-1} depicts C= O double bond stretching (Baloguna et al., 2024).

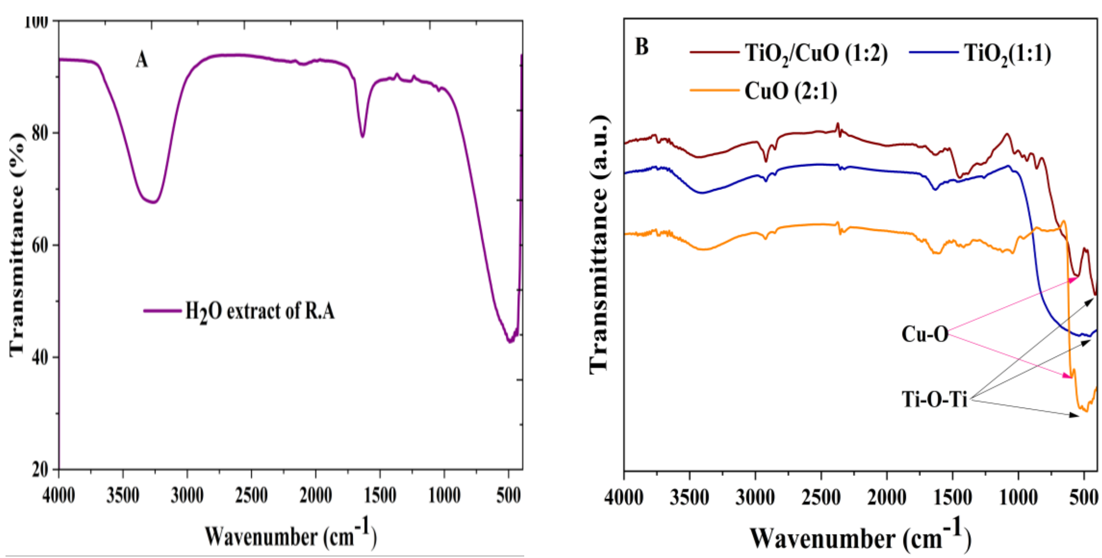

Figure 8. FTIR spectra of (A) R. abyssinica leaf extract and (B) TiO_2/CuO NCs.

4.5 Photoluminescence spectra analysis

The lifetime of photo-generated electron holes in semiconductors and the effectiveness of charge carrier transfer were both studied using photoluminescence (PL) emission spectra. PL spectra were also used in several investigations that showed a notable improvement in the separation of photo-generated carriers as shown in Figure 9. The TiO_2/CuO NC with (1:1) precursors ratio is represented by the lowest peak intensity in the figure, showing that the holes and electrons recombination reduced this ratio as compared to (2:1) and (1:2). The decreased electron-hole recombination improves the photocatalytic effectiveness of TiO_2/CuO NCs.

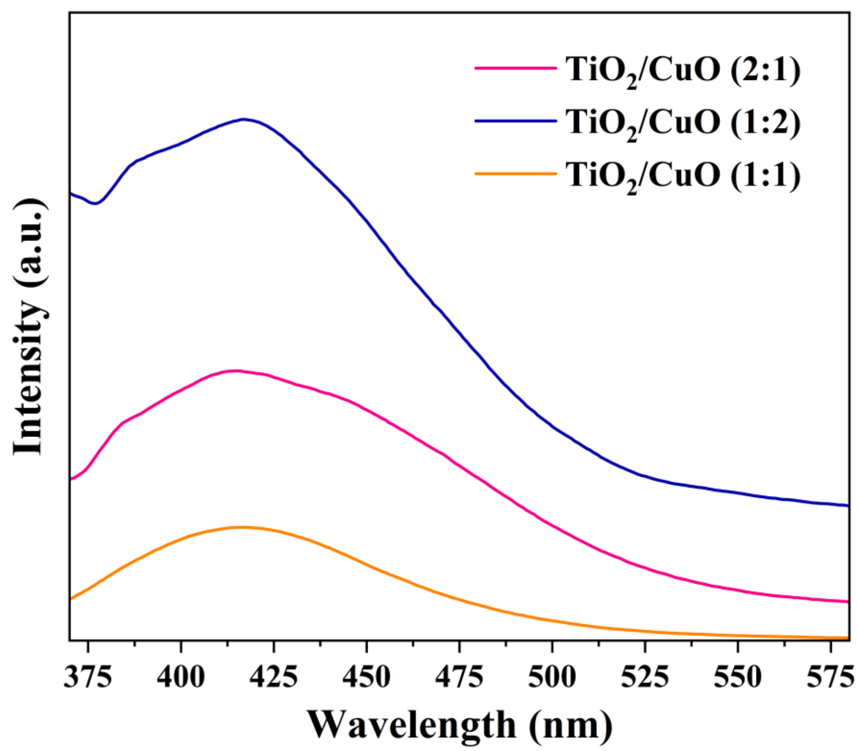

Figure 9. PL spectra of biosynthesized TiO_2/CuO nanocomposites.

4.6 Photocatalytic activity test

Photocatalytic performance optimization of different ratios of the biosynthesized TiO_2/CuO NCs was performed by the degradation of MB in an aqueous solution under light irradiation at a dye concentration of 10 ppm, catalyst dose of 20 mg, pH of 7, and a time interval of 80 minutes. MB shows a maximum absorption at about 664 nm. The photodegradation performance of the biosynthesized TiO_2 /CuO NCs with different ratios against MB was tested and the absorption spectra are shown in Figure 10 (A-C). Among the three ratios, TiO_2 /CuO (1:1) showed the highest decomposition of MB in an aqueous solution as indicated in Figure 10 C.

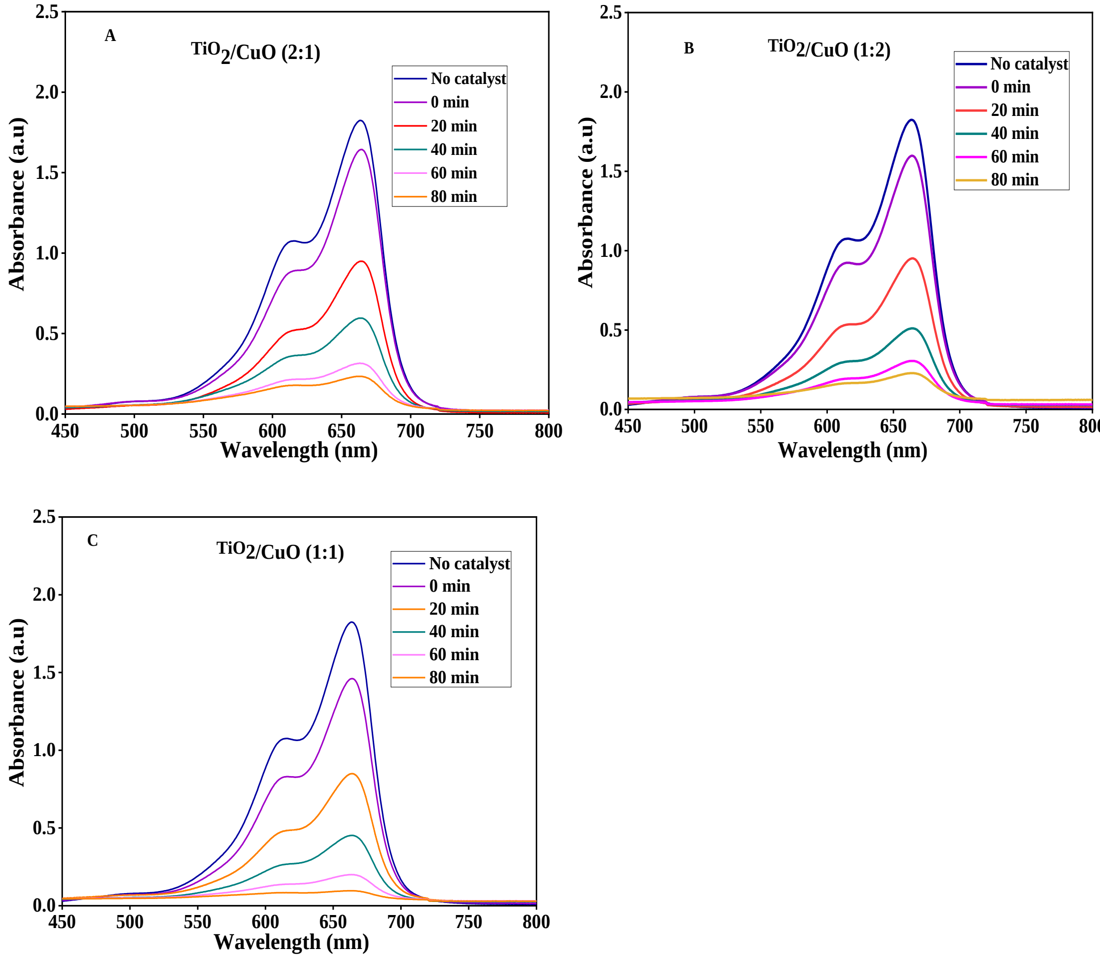

Figure 10. UV–visible spectra showing the reduction in the intensity of MB dye solution under light irradiation by using NCs TiO_2 /CuO with the ratio (2:1)(A), (1:2)(B), and (1:1)(C).

The photocatalytic activity observed where inversely related to the PL spectra intensity. This is related to an increase in the lifetime of photogenerated (e^- /h+) pairs of the lowest PL intensity of (1:1) (El Mragui et al., 2021).

The plot of $\ln(C/C_0)$ versus irradiation time (t) was explored using the pseudo-first-order rate constant for the degradation of MB**.** The plot of $\ln(C/C_0)$ Vs irradiation time as shown in Figure 11 gives the rate constant for the synthesized nanocomposites. The rate constant for TiO_2/CuO (2:1), TiO_2/CuO (1:2), and TiO_2/CuO (1:1) were found to be 0.0147, 0.0179, and 0.0223 min^{-1}, respectively. Among them, TiO_2/CuO (1:1) possesses the highest degradation rate constant. Plots of $\ln(C/C_0)$ versus irradiation time (*t*) for the pure and doped samples, show an approximated linear relationship between the two variables. This indicates that the photodegradation of MB follows a pseudo-first-order reaction (Nguyen et al., 2019).

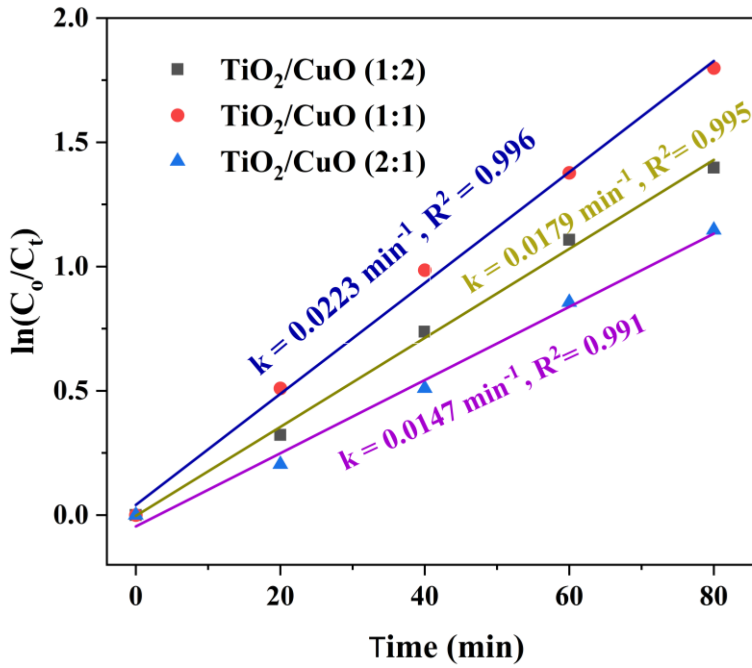

Figure 11. Plots of $\ln(C/C_0)$ vs. degradation times of MB different ratios of the NCs.

4.6.1 Effect of pH

The effect of pH was studied for the photocatalytic degradation of MB solution with TiO_2/CuO (1:1) catalyst based on the above optimization. To demonstrate the photocatalytic degradation of MB, different pH solutions of 4, 7, and 10 were used along with 20 mg of TiO_2/CuO (1:1) catalyst and 10 ppm of MB solution with corresponding time intervals of 0 to 80 minutes as shown in Figure 12.

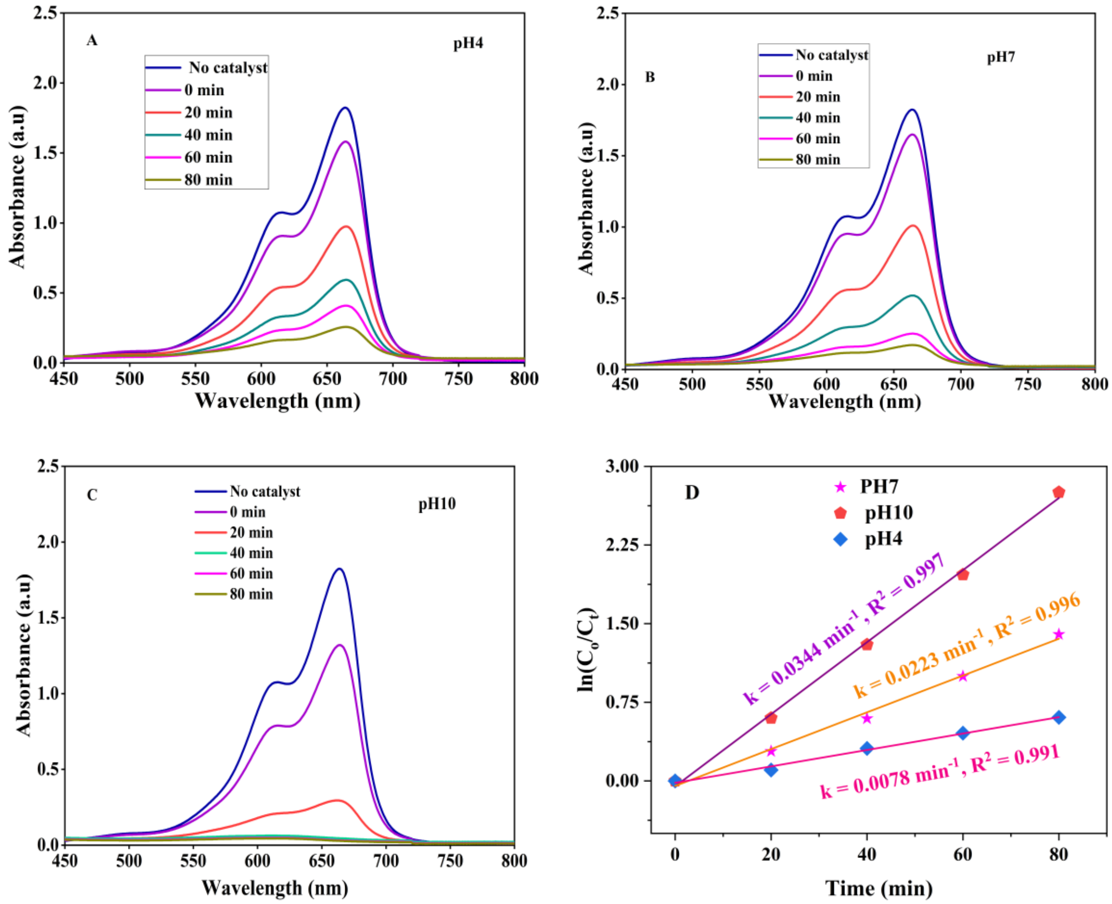

Figure 12. UV-visible spectra of MB with different pH of 4 (A), 7 (B), and 10 (C) and rate degradation (D) in the presence of TiO_2/CuO (1:1) NC at different pH.

The TiO_2/CuO (1:1) NC efficiency of photodegradation was tested at different pH environments. However, the degradation ability of the sample steadily increases from pH4 to pH10 with the rate constant values (K) of 0.0078, 0.0223, and 0.0344 min^{-1} at pH4, pH7, and pH10, respectively as shown in Figure 12D. This may be due to the variation in electrostatic forces between the catalyst surface and MB molecules at various pH levels. In an alkaline medium, the catalyst's surface is negatively charged while in an acidic medium, it is positively charged. MB is a cationic dye, so when it dissolves in water, its structure becomes positively charged. Therefore, the rate of MB degradation is higher in alkaline media due to an increase in opposite-charge interactions between the solution and catalyst surface (Prabakaran & Pillay, 2019).

4.6.2 Effect of Initial Dye Concentration

The effect of different initial concentrations of MB was tested for the photocatalytic activity with TiO_2/CuO (1:1) at pH10, catalyst dose of 20 mg, and the time intervals of 0 to 80 minutes as shown in Figure 13A-C.

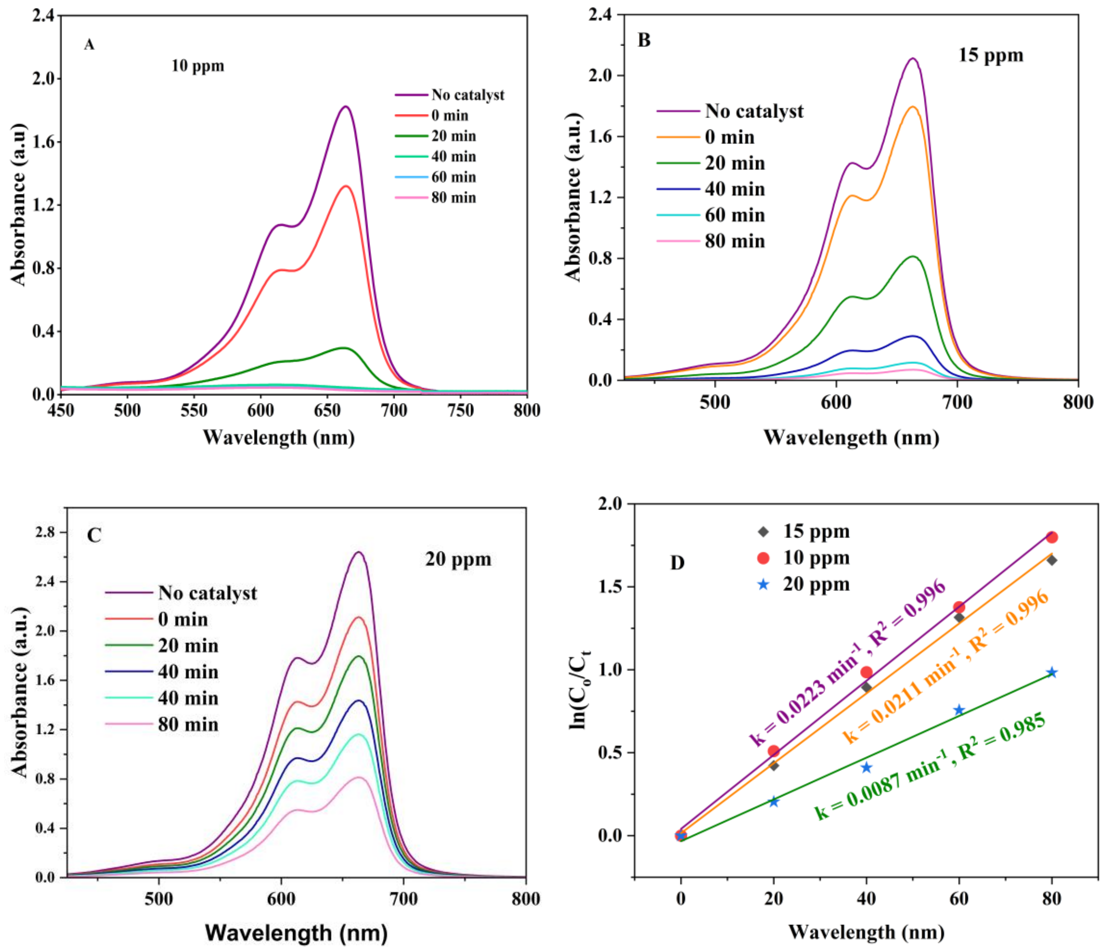

Figure 13. UV-visible spectra of MB with different initial concentrations of 10 ppm (A), 15 ppm (B), and 20 ppm (C) at pH10, 20 mg TiO_2/CuO (1:1) catalyst dose and with reaction time interval 0 to 80 minutes and the rate of degradation (D).

The effect of initial MB concentration was investigated by using 10 ppm, 15 ppm, and 20 ppm of MB concentration with 20 mg of 6 TiO_2/CuO (1:1) NC.

The results in Figure 13D show that the degradation efficiency is high at low concentrations of organic dyes and gradually decreases as the dye concentration increases. This is because the initial dye concentration increased indirectly, the excess of dye molecules will be adsorbed on the catalyst surface, so the active sites of the catalysts will be reduced. As the dye concentration increases, some hydroxyl radicals are required for the degradation of dye molecules and, the formation of hydroxyl radicals on the catalyst surface remains constant for a given light intensity, catalyst dose, and irradiation time. Therefore, the hydroxyl radicals produced are insufficient for the degradation of dye at high concentrations. Hence, photodegradation efficiency reduces as the concentration of dye increases (Isai & Shrivastava, 2019). The reaction rates were found to decrease with increasing MB concentration from the rate constant of 0.0223 min^{-1} for 10 ppm to 0.0087 min^{-1} for 20 ppm and followed the pseudo-first-order kinetic model.

4.6.3 Effect of Catalyst Dosage

Figure 14(A-D) shows the effect of the dosage of TiO_2/CuO (1:1) catalyst on the photocatalytic degradation of MB under light irradiation with time intervals of 0 to 80 minutes at pH10, 15 ppm of dye. The influence of the photo catalyst dosage on the degradation of MB using TiO_2/CuO (1:1) catalyst was studied by making the amount of photocatalyst 10 mg, 20 mg, and 30 mg with an initial MB concentration of 15 ppm. An increase in the degradation efficiency was observed with the increase in catalyst dosage. This is due to the exposure of more active sites on the photocatalyst, which adsorb more photons and produces more OH• radicals and positive holes under irradiation. These hydroxyl radicals and positive holes participate in the photocatalytic reaction, and thus, the rate of degradation of pollutants increases. At a lower dosage of catalyst, most of the irradiated light is directly transmitted from the solution, and a small part of it is consumed by the catalyst to perform. When the amount of catalyst is excessive, photocatalytic degradation decreases because the active molecules collide with the basic state molecules and lose their activity. Moreover, it should be noticed that the reduction in the percentage of degradation at higher catalyst loading may be related to increased scattering and turbidity effects, which does not allow the penetration of light into all available surfaces of particles (Çağlar Yılmaz et al., 2020; Reza et al., 2017).

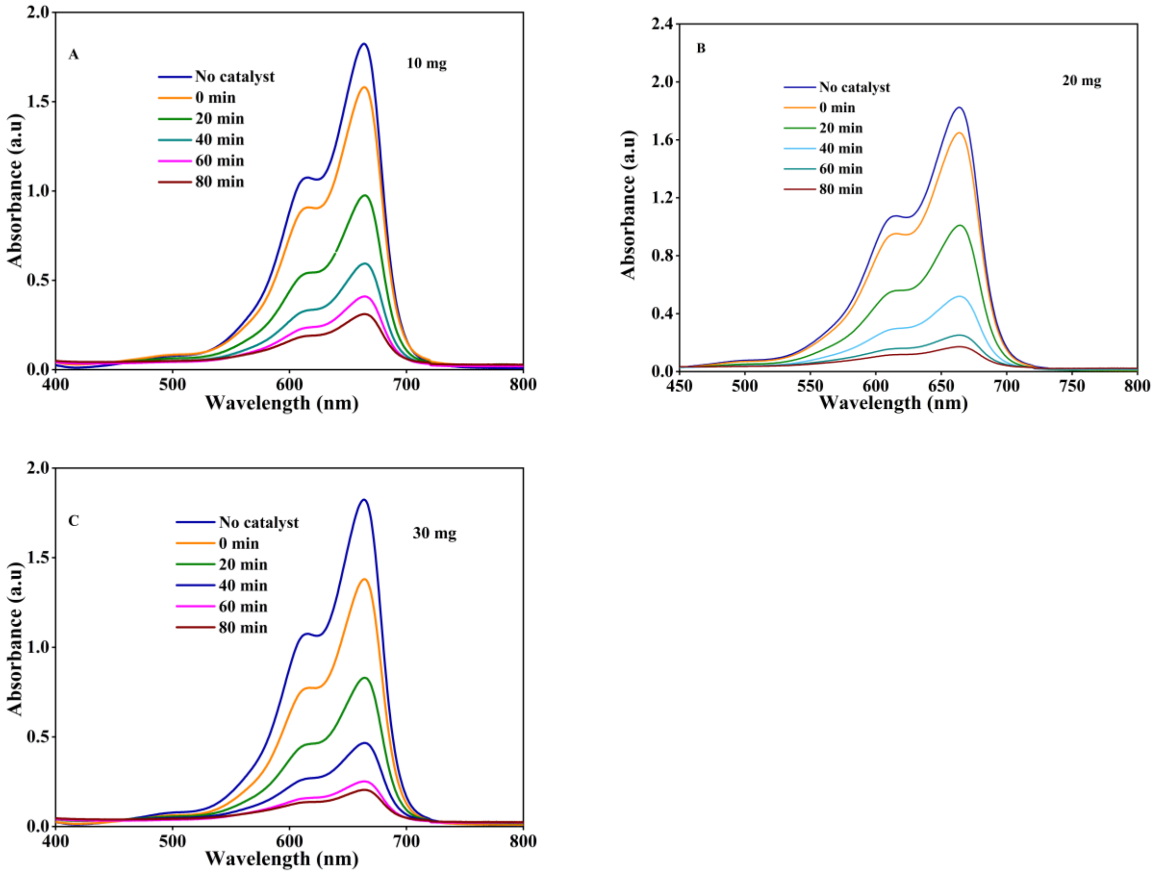

Figure 14. UV-visible spectra of MB with different catalysts of TiO_2/CuO (1:1) 10 mg (A), 20 mg (B), 30 mg (C), with reaction time intervals 0 to 80 minutes.

4.7 Reusability test

The recyclability and stability of photocatalysts are critical factors that significantly contribute to cost reduction while ensuring that these materials deliver consistent and effective performance in removing pollutants. In particular, the reusability of TiO_2/CuO NC has been studied extensively, demonstrating impressive stability across multiple cycles of use. The evaluation of their photocatalytic activity revealed notable results in terms of pollutant removal efficiency. Specifically, during the first testing cycle, the TiO_2/CuO NC achieved a remarkable pollutant removal rate of 94%. This high level of efficiency was only slightly diminished in subsequent cycles, with the second cycle recording a removal rate of 91.5%. The third cycle followed closely behind with a 90% removal rate, and by the fourth cycle, efficiency remained commendable at 89.3%. These results not only highlight the excellent stability of the TiO_2/CuO nanocomposite but also affirm its potential for practical applications in environmental remediation. The consistent performance throughout multiple cycles underscores the reliability of this photocatalyst, making it a promising option aiming to minimize operational costs while effectively addressing environmental pollutants. This data is illustrated in Figure 15, showcasing the gradual yet stable decline in photocatalytic efficiency across the tested cycles.

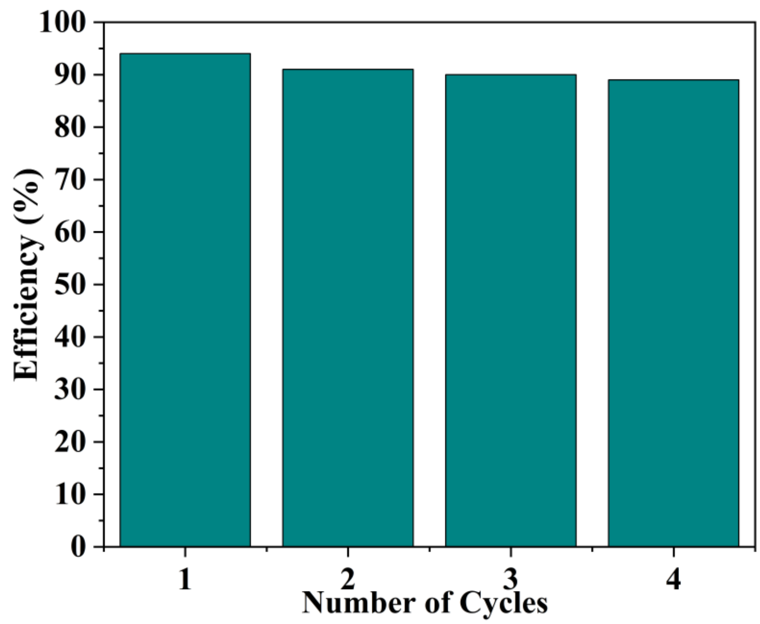

Figure 15. Reusability test of TiO_2/CuO NC for photodegradation of MB dye.

5 Conclusions

In the present study, the synthesis of TiO_2/CuO NCs was accomplished through a green synthetic method that employed Rosa Abyssinia leaves extract, acting as a reducing agent as well as a capping and stabilizing agent for the nanocomposites. To thoroughly assess the synthesized TiO_2/CuO NCs, an extensive evaluation was conducted focusing on their structural, thermal, optical, and crystallinity properties. This assessment utilized a range of characterization techniques, including photoluminescence (PL), ultraviolet-visible (UV-Vis) spectroscopy, Fourier-transform infrared spectroscopy (FTIR), and X-ray diffraction (XRD). Such comprehensive characterization is crucial for understanding the material properties and potential applications of nanocomposites in various fields. The average crystallite sizes of the biosynthesized nanocomposites were measured, revealing the dimensions of TiO_2/CuO in different ratios: the sample with a 1:1 ratio had an average crystallite size of 12.5 nm, the 1:2 ratio resulted in a size of 14 nm, and the 2:1 ratio exhibited a larger size of 17 nm. A further examination of the optical properties was carried out using UV-Vis diffuse reflectance spectroscopy (DRS), which provided insights into the energy band gaps of the synthesized nanocomposites. The estimated energy band gaps were found to be 2.31 eV for theTiO_2/CuO (2:1) composition, 2.65 eV for TiO_2/CuO (1:1), and 2.75 eV for TiO_2/CuO (1:2). These values are significant as they directly influence the photocatalytic activity of the materials. The photocatalytic degradation efficiency of the synthesized nanocomposites was evaluated by testing their performance against methylene blue (MB) dye in an aqueous solution. The results indicated that TiO_2/CuO (1:1) demonstrated a notable photocatalytic removal efficiency of 94% under optimized conditions. These conditions included an initial MB dye concentration of 15 ppm, a pH level of 10, a catalyst dosage of 20 mg, and a contact time of 80 minutes. Such high efficiency underscores the potential applicability of these nanocomposites in wastewater treatment and environmental remediation. Furthermore, the kinetic analysis conducted on the photocatalytic degradation of MB indicated that the reaction adhered well to a pseudo-first-order kinetic model, suggesting a predictable and quantifiable degradation process. The investigation into the reusability of the TiO_2/CuO (1:1) nanocomposite revealed its good stability over multiple cycles of use, which is an essential aspect for practical applications in sustainable environmental solutions.

6 References

Adyani, S. M., & Ghorbani, M. (2018). A comparative study of physicochemical and photocatalytic properties of visible light responsive Fe, Gd and P single and tri-doped TiO2 nanomaterials. *Journal of Rare Earths*, *36*(1), 72-85.

Agidew, M. G. (2022). Phytochemical analysis of some selected traditional medicinal plants in Ethiopia. *Bulletin of the National Research Centre*, *46*(1), 87.

Ahamed, S. T., Ghosh, A., Show, B., & Mondal, A. (2020). Fabrication of n-TiO 2/p-CuO thin-film heterojunction for efficient photocatalytic degradation of toxic organic dyes and reduction of metal ions in solution. *Journal of Materials Science: Materials in Electronics*, *31*, 16616-16633.

Ahmad, W., Jaiswal, K. K., & Soni, S. (2020). Green synthesis of titanium dioxide (TiO2) nanoparticles by using Mentha arvensis leaves extract and its antimicrobial properties. *Inorganic and Nano-Metal Chemistry*, *50*(10), 1032-1038.

Alizadeh, N., Shariati, S., & Besharati, N. (2017). Adsorption of crystal violet and methylene blue on azolla and fig leaves modified with magnetite iron oxide nanoparticles. *International journal of environmental research*, *11*, 197-206.

Alkaykh, S., Mbarek, A., & Ali-Shattle, E. E. (2020). Photocatalytic degradation of methylene blue dye in aqueous solution by MnTiO3 nanoparticles under sunlight irradiation. *Heliyon*, *6*(4), e03663.

Aloi, G. (2018). *Why look at plants?: The botanical emergence in contemporary art* (Vol. 5). Brill.

Alshaikh, H., Shawky, A., Mohamed, R., Knight, J. G., & Roselin, L. S. (2021). Solution-based synthesis of Co3O4/ZnO pn heterojunctions for rapid visible-light-driven oxidation of ciprofloxacin. *Journal of Molecular Liquids*, *334*, 116092.

Álvarez-Chimal, R., & Arenas-Alatorre, J. Á. (2023). Green synthesis of nanoparticles. A biological approach.

Anand, A. M., Raj, A., Adithya Nath, R., Salam, J. A., & Jayakrishnan, R. (2023). Self-powered UV photodetector based on self-assembled CuO and spin-coated ZnO heterostructure. *Journal of Materials Science*, *58*(27), 11000-11015.

Anigol, L. B., Charantimath, J. S., & Gurubasavaraj, P. M. (2017). Effect of concentration and pH on the size of silver nanoparticles synthesized by green chemistry. *Org. Med. Chem. Int. J*, *3*(5), 1-5.

Anjum, F., Shaban, M., Ismail, M., Gul, S., Bakhsh, E. M., Khan, M. A., Sharafat, U., Khan, S. B., & Khan, M. I. (2023). Novel Synthesis of CuO/GO Nanocomposites and Their Photocatalytic Potential in the Degradation of Hazardous Industrial Effluents. *ACS omega*, *8*(20), 17667-17681.

Annu, A. A., & Ahmed, S. (2018). Green synthesis of metal, metal oxide nanoparticles, and their various applications. *Handbook of Ecomaterials*, *2018*, 1-45.

Aravind, M., Amalanathan, M., & Mary, M. S. M. (2021). Synthesis of TiO 2 nanoparticles by chemical and green synthesis methods and their multifaceted properties. *SN Applied Sciences*, *3*(4), 1-10.

Aslam, A., Mehmood, U., Arshad, M. H., Ishfaq, A., Zaheer, J., Khan, A. U. H., & Sufyan, M. (2020). Dye-sensitized solar cells (DSSCs) as a potential photovoltaic technology for the self-powered internet of things (IoTs) applications. *Solar Energy*, *207*, 874-892.

Baek, Y.-W., & An, Y.-J. (2011). Microbial toxicity of metal oxide nanoparticles (CuO, NiO, ZnO, and Sb2O3) to Escherichia coli, Bacillus subtilis, and Streptococcus aureus. *Science of The Total Environment*, *409*(8), 1603-1608.

Bakatula, E. N., Richard, D., Neculita, C. M., & Zagury, G. J. (2018). Determination of point of zero charge of natural organic materials. *Environmental Science and Pollution Research*, *25*, 7823-7833.

Baloguna, S., Oyesholab, H., Belloa, S., & Ojoa, S. (2024). Ixora Coccinea Extract for Biosynthesis of Titanium Dioxide Nanoparticles: A Precursor for Organic Electronics. *Journal of Materials*, *2*(4), 279-287.

Bangari, R. S., Yadav, A., Bharadwaj, J., & Sinha, N. (2022). Boron nitride nanosheets incorporated polyvinylidene fluoride mixed matrix membranes for removal of methylene blue from aqueous stream. *Journal of Environmental Chemical Engineering*, *10*(1), 107052.

Bano, S., Sultana, S., & Sabir, S. (2020). Metal oxide nanostructured materials for water treatment: Prospectives and challenges. *Modern Age Waste Water Problems: Solutions Using Applied Nanotechnology*, 213-231.

Baumgarten, R., Ingale, P., Knemeyer, K., Naumann d'Alnoncourt, R., Driess, M., & Rosowski, F. (2022). Synthesis of High Surface Area—Group 13—Metal Oxides via Atomic Layer Deposition on Mesoporous Silica. *Nanomaterials*, *12*(9), 1458.

Baysal, G. (2020). The Components of Functional Nanosystems and Nanostructures. In *Smart Nanosystems for Biomedicine, Optoelectronics and Catalysis*. IntechOpen.

Bisht, S., Ghalwan, M., Oza, A. D., Saxena, K. K., & Prakash, C. (2023). Green synthesis of CuO/TiO2 nanocomposite based photo catalyst and its applications in treatment of waste water. *International Journal on Interactive Design and Manufacturing (IJIDeM)*, 1-6.

Blangetti, N., Freyria, F. S., Calviello, M. C., Ditaranto, N., Guastella, S., & Bonelli, B. (2023). Photocatalytic Degradation of Paracetamol under Simulated Sunlight by Four TiO2 Commercial Powders: An Insight into the Performance of Two Sub-Micrometric Anatase and Rutile Powders and a Nanometric Brookite Powder. *Catalysts*, *13*(2), 434.

Bopape, D. A., Mathobela, S., Matinise, N., Motaung, D. E., & Hintsho-Mbita, N. C. (2023). Green synthesis of CuO-TiO2 nanoparticles for the degradation of organic pollutants: physical, optical and electrochemical properties. *Catalysts*, *13*(1), 163.

Boretti, A., & Rosa, L. (2019). Reassessing the projections of the world water development report. *NPJ Clean Water*, *2*(1), 15.

Çağlar Yılmaz, H., Akgeyik, E., Bougarrani, S., El Azzouzi, M., & Erdemoğlu, S. (2020). Photocatalytic degradation of amoxicillin using Co-doped TiO2 synthesized by reflux method and monitoring of degradation products by LC–MS/MS. *Journal of Dispersion Science and Technology*, *41*(3), 414-425.

Cahino, A. M., Loureiro, R. G., Dantas, J., Madeira, V. S., & Fernandes, P. C. R. (2019). Characterization and evaluation of ZnO/CuO catalyst in the degradation of methylene blue using solar radiation. *Ceramics International*, *45*(11), 13628-13636.

Cao, H., Wang, R., Dou, K., Qiu, J., Peng, C., Tsidaeva, N., & Wang, W. (2023). High-efficiency adsorption removal of CR and MG dyes using AlOOH fibers embedded with porous CoFe2O4 nanoparticles. *Environmental Research*, *216*, 114730.

Celik, E., Gokcen, Z., Azem, N. A., Tanoglu, M., & Emrullahoglu, O. (2006). Processing, characterization and photocatalytic properties of Cu doped TiO2 thin films on glass substrate by sol–gel technique. *Materials Science and Engineering: B*, *132*(3), 258-265.

Chatterjee, S. (2018). Performance of Dye-Sensitized Solar Cells (DSSCs) Fabricated with Zinc Oxide (ZnO) Nanpowders and Nanorods. *Journal of Materials Engineering and Performance*, *27*(6), 2713-2718.

Chi, N., & Wang, Y. (2022). Synthesis and application of CuO-TiO2 hybrid nanostructures as Photocatalytst for degradation of p-nitrophenol in wastewater. *INTERNATIONAL JOURNAL OF ELECTROCHEMICAL SCIENCE*, *17*(10).

Danish, M. S. S., Estrella, L. L., Alemaida, I. M. A., Lisin, A., Moiseev, N., Ahmadi, M., Nazari, M., Wali, M., Zaheb, H., & Senjyu, T. (2021). Photocatalytic applications of metal oxides for sustainable environmental remediation. *Metals*, *11*(1), 80.

Dubale, S., Kebebe, D., Zeynudin, A., Abdissa, N., & Suleman, S. (2023). Phytochemical screening and antimicrobial activity evaluation of selected medicinal plants in Ethiopia. *Journal of Experimental Pharmacology*, 51-62.

Ealia, S. A. M., & Saravanakumar, M. (2017). A review on the classification, characterisation, synthesis of nanoparticles and their application. IOP Conference Series: Materials Science and Engineering,

El-Ghamri, H. S., Taya, S. A., El-Agez, T. M., Al-Kahlout, A. M., Al Dahoudi, N., & Abdel-Latif, M. S. (2015). Natural dyes as photosensitizers for dye-sensitized solar cells.

El Mragui, A., Zegaoui, O., Daou, I., & Esteves da Silva, J. C. G. (2021). Preparation, characterization, and photocatalytic activity under UV and visible light of Co, Mn, and Ni mono-doped and (P, Mo) and (P, W) co-doped TiO 2 nanoparticles: A comparative study. *Environmental Science and Pollution Research*, *28*, 25130-25145.

El Shafey, A. M. (2020). Green synthesis of metal and metal oxide nanoparticles from plant leaf extracts and their applications: A review. *Green Processing and Synthesis*, *9*(1), 304-339.

Elbadawy, H. A., Elhusseiny, A. F., Hussein, S. M., & Sadik, W. A. (2023). Sustainable and energy-efficient photocatalytic degradation of textile dye assisted by ecofriendly synthesized silver nanoparticles. *Scientific Reports*, *13*(1), 2302.

Etape, E. P., Ngolui, L. J., Foba-Tendo, J., Yufanyi, D. M., & Namondo, B. V. (2017). Synthesis and characterization of CuO, TiO2, and CuO-TiO2 mixed oxide by a modified oxalate route. *J. Appl. Chem*, *2017*, 1-10.

Feiona, T. A., Sabeena, G., Bagavathy, M. S., Pushpalaksmi, E., Jenson Samraj, J., & Annadurai, G. (2021). Recent Advances in the Synthesis and Characterization of Nanoparticles: A Green Adeptness for Photocatalytic and Antibacterial Activity. *Nature Environment & Pollution Technology*, *20*(2).

García-Salinas, M. J., & Ariza, M. J. (2019). Optimizing a simple natural dye production method for dye-sensitized solar cells: Examples for betalain (bougainvillea and beetroot extracts) and anthocyanin dyes. *Applied Sciences*, *9*(12), 2515.

Gebremedhin, B. R., Tamtam, M. R., Koutavarapu, R., & Shim, J. (2023). Eco-friendly synthesis of CuO nanoparticles induced by Var. adoensis and its high photocatalytic ability and recyclability. *Journal of Materials Science: Materials in Electronics*, *34*(8), 703.

Gnanasangeetha, D., & Suresh, M. (2020). A Review on Green Synthesis of Metal and Metal Oxide Nanoparticles. *Nature Environment and Pollution Technology*, *19*(5), 1789-1800.

Gómez-Pastora, J., Dominguez, S., Bringas, E., Rivero, M. J., Ortiz, I., & Dionysiou, D. D. (2017). Review and perspectives on the use of magnetic nanophotocatalysts (MNPCs) in water treatment. *Chemical Engineering Journal*, *310*, 407-427.

Gou, X., & Guo, Z. (2019). Hybrid hydrophilic–hydrophobic CuO@ TiO2-coated copper mesh for efficient water harvesting. *Langmuir*, *36*(1), 64-73.

Gouasmia, A., Zouaoui, E., Mekkaoui, A. A., Haddad, A., & Bousba, D. (2022). Highly efficient photocatalytic degradation of malachite green dye over copper oxide and copper cobaltite photocatalysts under solar or microwave irradiation. *Inorganic Chemistry Communications*, *145*, 110066.

Halake, K., & Lee, J. (2017). Functional hyaluronic acid conjugates based on natural polyphenols exhibit antioxidant, adhesive, gelation, and self-healing properties. *Journal of Industrial and Engineering Chemistry*, *54*, 44-51.

Hassanzadeh, H., Salem, A., & Salem, S. (2023). Fabrication of MgO powder through ultrasound-assisted precipitation for uptake of reactive dyes from wastewater: Change in porous structure for efficient adsorption. *Inorganic Chemistry Communications*, *155*, 111004.

Hosseini, H., Zirakjou, A., McClements, D. J., Goodarzi, V., & Chen, W.-H. (2022). Removal of methylene blue from wastewater using ternary nanocomposite aerogel systems: Carboxymethyl cellulose grafted by polyacrylic acid and decorated with graphene oxide. *Journal of Hazardous Materials*, *421*, 126752.

Isai, K. A., & Shrivastava, V. S. (2019). Photocatalytic degradation of methylene blue using ZnO and 2% Fe–ZnO semiconductor nanomaterials synthesized by sol–gel method: a comparative study. *SN Applied Sciences*, *1*, 1-11.

Ismail, H. H., Hasoon, S. A., & Saheb, E. J. (2019). The anti-Leishmaniasis activity of green synthesis silver oxide nanoparticles. *Annals of Tropical Medicine and Health*, *22*, 28-38.

Jalab, J., Abdelwahed, W., Kitaz, A., & Al-Kayali, R. (2021). Green synthesis of silver nanoparticles using aqueous extract of Acacia cyanophylla and its antibacterial activity. *Heliyon*, *7*(9), e08033.

Janczarek, M., & Kowalska, E. (2017). On the origin of enhanced photocatalytic activity of copper-modified titania in the oxidative reaction systems. Catalysts, 7 (11), 317. In.

Javed, A., QAMMAR, M., Khurram, R., Nisa, Z., & Nasir, H. (2021). Visible Light Active Nitrogen and Cobalt Co-doped TiO2 Nanoparticles: Synthesis, Characterization and Photocatalytic Activity.

Kannan, K., Radhika, D., Gnanasangeetha, D., Lakkaboyana, S. K., Sadasivuni, K. K., Gurushankar, K., & Hanafiah, M. M. (2021). Photocatalytic and antimicrobial properties of microwave synthesized mixed metal oxide nanocomposite. *Inorganic Chemistry Communications*, *125*, 108429.

Khan, M. D., Singh, A., Khan, M. Z., Tabraiz, S., & Sheikh, J. (2023). Current perspectives, recent advancements, and efficiencies of various dye-containing wastewater treatment technologies. *Journal of Water Process Engineering*, *53*, 103579.

Khoroshko, L., Borisenko, V., Baltrukovich, P., Nurmonov, S., & Ruzimuradov, O. (2023). One-step sol-gel fabrication of TiO2/(CuO+ Cu2O) photocatalysts. *Journal of Sol-Gel Science and Technology*, *108*(2), 320-324.

Kubiak, A., Bielan, Z., Kubacka, M., Gabała, E., Zgoła-Grześkowiak, A., Janczarek, M., Zalas, M., Zielińska-Jurek, A., Siwińska-Ciesielczyk, K., & Jesionowski, T. (2020). Microwave-assisted synthesis of a TiO2-CuO heterojunction with enhanced photocatalytic activity against tetracycline. *Applied Surface Science*, *520*, 146344.

Kumar, S., Saralch, S., Jabeen, U., & Pathak, D. (2020). Metal oxides for energy applications. In *Colloidal Metal Oxide Nanoparticles* (pp. 471-504). Elsevier.

Kumari, H., Sonia, Suman, Ranga, R., Chahal, S., Devi, S., Sharma, S., Kumar, S., Kumar, P., & Kumar, S. (2023). A Review on Photocatalysis Used For Wastewater Treatment: Dye Degradation. *Water, Air, & Soil Pollution*, *234*(6), 349.

Low, J., Cheng, B., & Yu, J. (2017). Surface modification and enhanced photocatalytic CO2 reduction performance of TiO2: a review. *Applied Surface Science*, *392*, 658-686.

Lu, D., Zelekew, O. A., Abay, A. K., Huang, Q., Chen, X., & Zheng, Y. (2019). Synthesis and photocatalytic activities of a CuO/TiO 2 composite catalyst using aquatic plants with accumulated copper as a template. *RSC advances*, *9*(4), 2018-2025.

Lu, X., Wang, H., Chen, J., Yang, L., Hu, T., Wu, F., Fu, J., & Chen, Z. (2022). Negatively charged hollow crosslinked aromatic polymer fiber membrane for high-efficiency removal of cationic dyes in wastewater. *Chemical Engineering Journal*, *433*, 133650.

Machut, C., Kania, N., Léger, B., Wyrwalski, F., Noël, S., Addad, A., Monflier, E., & Ponchel, A. (2020). Fast Microwave Synthesis of Gold-Doped TiO2 Assisted by

Modified Cyclodextrins for Photocatalytic Degradation of Dye and Hydrogen Production. *Catalysts*, *10*(7), 801.

Martins, L. R., Soares, L. C., Gurgel, L. V. A., & Gil, L. F. (2022). Use of a new zwitterionic cellulose derivative for removal of crystal violet and orange II from aqueous solutions. *Journal of Hazardous Materials, 424*, 127401.

Matheyarasu, R., Seshadri, B., Bolan, N. S., & Naidu, R. (2014). Impacts of abattoir waste-water irrigation on soil fertility and productivity.

May-Masnou, A., Soler, L., Torras, M., Salles, P., Llorca, J., & Roig, A. (2018). Fast and simple microwave synthesis of TiO2/Au nanoparticles for gas-phase photocatalytic hydrogen generation. *Frontiers in chemistry*, *6*, 110.

Meena, J., Kumaraguru, N., Sami veerappa, N., Shin, P.-k., Tatsugi, J., Kumar, A. S., & Santhakumar, K. (2023). Copper oxide nanoparticles fabricated by green chemistry using Tribulus terrestris seed natural extract-photocatalyst and green electrodes for energy storage device. *Scientific Reports*, *13*(1), 22499.

Muniz, E. C., Góes, M. S., Silva, J. J., Varela, J. A., Joanni, E., Parra, R., & Bueno, P. R. (2011). Synthesis and characterization of mesoporous TiO2 nanostructured films prepared by a modified sol–gel method for application in dye solar cells. *Ceramics International*, *37*(3), 1017-1024.

Murthy, S., Effiong, P., & Fei, C. C. (2020). Metal oxide nanoparticles in biomedical applications. In *Metal oxide powder technologies* (pp. 233-251). Elsevier.

Muzakki, A., Shabrany, H., & Saleh, R. (2016). Synthesis of ZnO/CuO and TiO2/CuO nanocomposites for light and ultrasound assisted degradation of a textile dye in aqueous solution. AIP Conference Proceedings,

Nguyen, L. T., Nguyen, L. T., Manh, N. C., Quoc, D. N., Quang, H. N., Nguyen, H. T., Nguyen, D. C., & Bach, L. G. (2019). A facile synthesis, characterization, and photocatalytic activity of magnesium ferrite nanoparticles via the solution combustion method. *Journal of Chemistry*, *2019*, 1-8.

Nyamukamba, P., Okoh, O., Mungondori, H., Taziwa, R., & Zinya, S. (2018). Synthetic methods for titanium dioxide nanoparticles: a review. *Titanium Dioxide—Material for a Sustainable Environment; Yang, D., Ed*, 151-175.

Oloya, B., Namukobe, J., Ssengooba, W., Afayoa, M., & Byamukama, R. (2022). Phytochemical screening, antimycobacterial activity and acute toxicity of crude extracts of selected medicinal plant species used locally in the treatment of tuberculosis in Uganda. *Tropical medicine and health*, *50*(1), 16.

Osonga, F. J., Akgul, A., Yazgan, I., Akgul, A., Eshun, G. B., Sakhaee, L., & Sadik, O. A. (2020). Size and shape-dependent antimicrobial activities of silver and gold nanoparticles: A model study as potential fungicides. *Molecules*, *25*(11), 2682.

Pandit, B., & Sankapal, B. R. (2021). Chemically processed metal oxides for sensing application: Heterojunction room temperature LPG sensor. In *Chemically Deposited Nanocrystalline Metal Oxide Thin Films: Synthesis, Characterizations, and Applications* (pp. 765-805). Springer.

Patra, J. K., & Baek, K.-H. (2014). Green nanobiotechnology: factors affecting synthesis and characterization techniques. *Journal of Nanomaterials*, *2014*.

Pattnaik, A., Sahu, J., Poonia, A. K., & Ghosh, P. (2023). Current perspective of nano-engineered metal oxide based photocatalysts in advanced oxidation processes for degradation of organic pollutants in wastewater. *Chemical Engineering Research and Design*.

Paydar, S., Akbar, N., Shi, Q., & Wu, Y. (2021). Developing cuprospinel CuFe2O4–ZnO semiconductor heterostructure as a proton conducting electrolyte for advanced fuel cells. *International Journal of Hydrogen Energy*, *46*(15), 9927-9937.

Piaskowski, K., Świderska-Dąbrowska, R., & Zarzycki, P. K. (2018). Dye removal from water and wastewater using various physical, chemical, and biological processes. *Journal of AOAC International*, *101*(5), 1371-1384.

Prabakaran, E., & Pillay, K. (2019). Synthesis of N-doped ZnO nanoparticles with cabbage morphology as a catalyst for the efficient photocatalytic degradation of methylene blue under UV and visible light. *Rsc Advances*, *9*(13), 7509-7535.

Ramírez, S., Wang, J., Valenzuela, M., Chen, L., & Dalai, A. (2020). CuO@ TiO2 and NiO@ TiO2 core-shell catalysts for hydrogen production from the photocatalytic reforming of glycerol aqueous solution. *Journal of applied research and technology*, *18*(6), 390-409.

Ramutshatsha-Makhwedzha, D., & Nomngongo, P. N. (2022). Application of ultrafiltration membrane technology for removal of dyes from wastewater. *Membrane Based Methods for Dye Containing Wastewater: Recent Advances*, 37-47.

Rana, A., Pathak, S., Kumar, K., Kumari, A., Chopra, S., Kumar, M., Kamil, D., Srivastava, R., Kim, S.-K., & Verma, R. (2024). Multifaceted Properties of TiO2 Nanoparticles Synthesized via Mangifera indica and Azadirachta indica Plant Extracts: Antimicrobial, Antioxidant, and Non-linear Optical Investigations for Sustainable Agriculture Applications. *Materials Advances*.

Rao, M., Ravindranadh, K., & Shekhawat, M. (2016). Structural and electrical properties of TiO2 thin films. AIP Conference Proceedings,

Reza, K. M., Kurny, A., & Gulshan, F. (2017). Parameters affecting the photocatalytic degradation of dyes using TiO 2: a review. *Applied Water Science*, *7*, 1569-1578.

Rezaei, M., Mengelizadeh, N., Berizi, Z., Salehnia, S., Asgari, M., & Balarak, D. (2023). Synthesis of MMT− CuFe2O4 Composite as a Peroxymonosulfate Activator for the Degradation of Reactive Black 5. *ChemistrySelect*, *8*(2), e202201729.

Roy, J. (2022). The synthesis and applications of TiO2 nanoparticles derived from phytochemical sources. *Journal of Industrial and Engineering Chemistry*, *106*, 1-19.

Saha, K., Proma, R. Z., & Khan, N. (2020). Phytochemical screening of plant extracts and GC-MS analysis of n-hexane extract of the leaves of Cassia alata linn. *J Phytopharmacol*, *9*(5), 342-347.

Saleh, T. A. (2020). Nanomaterials: Classification, properties, and environmental toxicities. *Environmental Technology & Innovation*, 101067.

Salem, B. B., Essalah, G., Ameur, S. B., Duponchel, B., Guermazi, H., Guermazi, S., & Leroy, G. (2023). Synthesis and comparative study of the structural and optical properties of binary ZnO-based composites for environmental applications. *RSC advances*, *13*(9), 6287-6303.

Sayed, M. E., Ghouch, N. E., Younes, G., Noun, M., & Awad, R. (2024). Tailoring the Structural, Optical and Anti-corrosion Effect of Synthesized Sn-Doped CuO

Nanoparticles on Mild Steel in 0.5 M HCl Solution. *Journal of Materials Engineering and Performance*, 1-16.

Sayyed, S. G., Shaikh, A. V., Shinde, U. P., Hiremath, P., & Naik, N. (2023). Copper oxide-based high-performance symmetric flexible supercapacitor: potentiodynamic deposition. *Journal of Materials Science: Materials in Electronics*, *34*(17), 1361.

Selihin, N. M., & Tay, M. G. (2022). A review on future wastewater treatment technologies: micro-nanobubbles, hybrid electro-Fenton processes, photocatalytic fuel cells, and microbial fuel cells. *Water Science and Technology*, *85*(1), 319-341.

Sethy, N. K., Arif, Z., Mishra, P. K., & Kumar, P. (2020). Green synthesis of TiO2 nanoparticles from Syzygium cumini extract for photo-catalytic removal of lead (Pb) in explosive industrial wastewater. *Green Processing and Synthesis*, *9*(1), 171-181.

Shanaj, B., & John, X. (2016). Effect of calcination time on structural, optical and antimicrobial properties of nickel oxide nanoparticles. *J. Theor. Comput. Sci*, *3*(2), 149-159.

Shawky, A. M., Elshypany, R., El Sharkawy, H. M., Mubarak, M. F., & Selim, H. (2024). Emerald eco-synthesis: harnessing oleander for green silver nanoparticle production and advancing photocatalytic MB degradation with TiO2&CuO nanocomposite. *Scientific Reports*, *14*(1), 2456.

Singh, J., Dutta, T., Kim, K.-H., Rawat, M., Samddar, P., & Kumar, P. (2018). 'Green'synthesis of metals and their oxide nanoparticles: applications for environmental remediation. *Journal of Nanobiotechnology*, *16*(1), 1-24.

Solano, R., Maestre, D., Mueses, M., & Herrera, A. (2023). TiO2-CuO heterojunction nanoparticles synthesized by green chemistry supported on beach sand granules: optical, morphological and structural characterization. *Nano-Structures & Nano-Objects*, *35*, 101024.

Song, Y. Z., Liu, Z. J., Qi, B. X., Li, M., Xie, J., & Song, W. H. (2021). Facile Synthesis of Micro CuO Crystals for Li Ion Full Battery. *Journal of Inorganic and Organometallic Polymers and Materials*, *31*(11), 4434-4439.

Srivastava, R. (2012). Synthesis and characterization techniques of nanomaterials. *International Journal of Green Nanotechnology*, *4*(1), 17-27.

Sronsri, C., Kongpop, U., & Sittipol, W. (2021). Analyses of vibrational spectroscopy, thermal property and salt solubility of magnetized water. *Journal of Molecular Liquids*, *323*, 114613.

Tauc, J., Grigorovici, R., & Vancu, A. (1966). Optical properties and electronic structure of amorphous germanium. *physica status solidi (b)*, *15*(2), 627-637.

Thakur, S., & Mandal, S. K. (2020). Morphology engineering of ZnO nanorod arrays to hierarchical nanoflowers for enhanced photocatalytic activity and antibacterial action against Escherichia coli. *New Journal of Chemistry*, *44*(27), 11796-11807.

Wang, J. C., Hill, S. P., Dilbeck, T., Ogunsolu, O. O., Banerjee, T., & Hanson, K. (2018). Multimolecular assemblies on high surface area metal oxides and their role in interfacial energy and electron transfer. *Chemical Society Reviews*, *47*(1), 104-148.

YILDIRIM, N., Serin, T., & Serin, N. (2010). Investigation of a p-CuO/n-TiO2 thin film heterojunction fabricated by the sol-gel process. *Journal of Optoelectronics and Advanced Materials*, *12*(May 2010), 1153-1156.

Yitagesu, G. B., Leku, D. T., & Workneh, G. A. (2023). Green Synthesis of TiO2 Using Impatiens rothii Hook. f. Leaf Extract for Efficient Removal of Methylene Blue Dye. *ACS omega*.

Yohannis, S. W., Asfaw, Z., & Kelbessa, E. (2018). Ethnobotanical study of medicinal plants used by local people in menz gera midir district, north shewa zone, amhara regional state, Ethiopia. *Journal of Medicinal Plants Research*, *12*(21), 296-314.

Zazouli, M. A., & Kalankesh, L. R. (2017). Removal of precursors and disinfection by-products (DBPs) by membrane filtration from water; a review. *Journal of Environmental Health Science and Engineering*, *15*, 1-10.

Zhang, Q., Zhang, K., Xu, D., Yang, G., Huang, H., Nie, F., Liu, C., & Yang, S. (2014). CuO nanostructures: synthesis, characterization, growth mechanisms, fundamental properties, and applications. *Progress in Materials Science*, *60*, 208-337.